Pigment composition and photoprotection of Arctic sea ice algae during spring

Virginie Galindo, Michel Gosselin, Johann Lavaud, C J Mundy, Brent Else, Jens Ehn, Marcel Babin, Søren Rysgaard

Pigment composition and photoprotection of Arctic sea ice algae during spring

Virginie Galindo[1,*], Michel Gosselin[2], Johann Lavaud[3], C. J. Mundy[1], Brent Else[4], Jens Ehn[1], Marcel Babin[3], Søren Rysgaard[1,5,6]

[1]Centre for Earth Observation Science, Faculty of Environment, Earth and Resources, University of Manitoba, Winnipeg, Manitoba R3T 2N2, Canada

[2]Institut des sciences de la mer de Rimouski, Université du Québec à Rimouski, Rimouski, Québec G5L 3A1, Canada

[3]UMI 3376 TAKUVIK, Département de biologie, CNRS/Université Laval, Québec-Océan, Québec, Québec G1V 0A6, Canada

[4]Department of Geography, University of Calgary, Calgary, Alberta T2N 1N4, Canada

[5]Arctic Research Centre, Aarhus University, 8000 Aarhus, Denmark

[6]Greenland Climate Research Centre, Greenland Institute of Natural Resources, PO Box 570, 3900 Nuuk, Greenland

*Corresponding author: virginie.galindo@gmail.com

ABSTRACT: From the beginning of spring to the melt period, ice algae in the bottom of Arctic sea ice experience a large irradiance range, varying from <0.1% up to 25 or 30% of the incoming visible radiation. The increase in spring is usually rapid, with a varying photoacclimative response by bottom ice algae to protect themselves against excess light, such as changes in cellular pigment composition. This study focused on the temporal variation in pigment composition of bottom ice algae under 2 contrasting snow depths (thin and thick) during spring.

Controlled experiments were also carried out to investigate the photoprotective capacity of ice algae to relatively high irradiances during a short-term period (<6 h). Bottom ice algae were able to photoacclimate rapidly and effectively to irradiance ranging from 10 to 100 µmol photons m^{-2} s^{-1}. However, we observed contrasting responses in photoacclimation depending on the ice algal community composition and their light history. Our experimental results suggest that the xanthophyll cycle (diadinoxanthin to diatoxanthin conversion) and D1-protein recycling play an important role in stabilizing photoprotection in ice algae. In addition, bottom ice algae likely employed a 'cellular light-exposure memory' strategy in order to improve their photoacclimative response to changing light exposure. According to our data, this process could be maintained over at least 2 wk. Hence, ice algae may be more resilient to varying light conditions than previously thought, and may be well-adapted for the expected future light regime changes associated with variability in snow and sea ice cover.

KEY WORDS: Arctic · Snow melt · Ice algae · Pigments · Photoacclimation · Light memory

INTRODUCTION

The ice algal community resides mostly in the bottom 10 cm of sea ice (Smith et al. 1990, Riedel et al. 2008, Juhl et al. 2011) and is largely dominated by diatoms (Poulin et al. 2011), a very abundant and productive group of unicellular algae (Malviya et al. 2016). Diatoms are successfully adapted to polar conditions due to their unique low-light acclimation (Petrou et al. 2016, Lacour et al. 2017). Ice algae represent the initial and most significant source of primary production during the winter–spring transition in Arctic waters. They contribute 5–20% of total marine primary production in Arctic seasonally ice-covered waters (e.g. Michel et al. 2006, Arrigo et al. 2010, Loose et al. 2011) and >50% in perennially ice-covered waters (Legendre et al. 1992, Gosselin et al. 1997). Primary production of ice algae is influenced by many environmental variables such as temperature (Arrigo & Sullivan 1992), salinity (Ryan et al. 2004), and nutrient availability (Lizotte & Sullivan 1992, Lavoie et al. 2005), but mainly by irradiance in the range of photosynthetically active radiation (E_{PAR}; 400 to 700 nm), which is principally regulated by the thickness of snow and ice cover (Mundy et al. 2005, Aumack & Juhl 2015) in addition to the annual cycle and cloudiness. E_{PAR} reaching the bottom of first-year sea ice is often <1% of incident irradiance (Arrigo et al. 1993, Lazzara et al. 2007) at the beginning of spring, and thus the ice algal community is adapted to perform photosynthesis under very low

irradiance (e.g. Cota 1985, Johnsen & Hegseth 1991, Kühl et al. 2001). However, the rapid increase in light intensity and day length from winter to the spring melt period (Sakshaug & Slagstad 1991) results in a rapid increase in E_{PAR} of up to 25 or 30% of incident irradiance at the bottom ice (Perovich 2005, Campbell et al. 2014), exposing the ice algae to a large range of E_{PAR}. Light conditions can also change rapidly on a daily basis, mainly due to opposite and/or cumulative effects of melting and storms (rain or snow) that modify the snow cover thickness and optical properties. Furthermore, the acceleration of global warming in the Arctic affects snow and sea ice cover. Snow cover declined by 40% between 1989 and 2009 (Screen & Simmonds 2012, Overland et al. 2014) and during some periods, precipitation has switched from snow to rain (Comiso & Hall 2014), while sea-ice extent has retreated by 45% in the last 3 decades (Screen et al. 2011, Stroeve et al. 2012). All of these changes, accompanied by an earlier melt onset (Markus et al. 2009), are expected to increase the E_{PAR} levels transmitted through the sea-ice cover. This increase in transmitted E_{PAR} is foreseen to enhance ice algal biomass (Poulin et al. 2011) and production (Wassmann et al. 2011), but ice algae may also face light stress (Leu et al. 2016, Petrou et al. 2016) which may be of importance since they are adapted to very low light levels.

In order to sustain photosynthesis under changing light conditions, ice algae use some photobehavioral (i.e. vertical migration in pennate diatoms; Aumack et al. 2014) and photophysiological features described as photoprotection and photoacclimation. These photoprotective mechanisms allow algae to minimize oxidative photodamage generated by excess light exposure, and specifically to maintain photosystem II (PSII) photochemistry. They include changes in cellular photosynthetic and photoprotective pigment composition (Alou-Font et al. 2013), with an increase in antioxidant carotenes and xanthophylls depending on incident irradiance. On shorter time scales (i.e. <1 h) of light fluctuations, the most important photoprotective processes are the repair of damaged PSII (Petrou et al. 2010) and thermal dissipation of excess energy (Goss & Lepetit 2015). This process comprises a fast (seconds to minutes) enzymatic light-driven conversion of xanthophyll cycle (XC) pigments (Goss & Jakob 2010). In diatoms, the XC consists of the de-epoxidation of diadinoxanthin (DD) to diatoxanthin (DT) (Brunet et al. 2011, Kuczynska et al. 2015). In polar conditions, the XC is very important for optimizing algal photosynthetic activity during the spring–summer transition when

transmitted irradiance at the ice–water interface increases (Kashino et al. 2002, Katayama & Taguchi 2013, Ha et al. 2016, Katayama et al. 2017).

As bottom ice algae strongly contribute to Arctic marine primary production during spring, several studies have described their photophysiological responses to a change in E_{PAR} levels from winter to spring (e.g. Gosselin et al. 1985, Barlow et al. 1988, Kudoh et al. 1997, Manes & Gradinger 2009), through the spring season (e.g. Michel et al. 1988, Cota & Horne 1989, Ban et al. 2006, Alou-Font et al. 2013) and from spring to summer (Rysgaard et al. 2001), with a special focus on the potential deleterious effects of ultraviolet radiation (UVR) (Enberg et al. 2015, Leu et al. 2016). A few works have also focused on the impact of change in snow cover on the photoacclimation of ice algae (Juhl & Krembs 2010, Lund-Hansen et al. 2014), but little is known about their capacity to acclimate to rapid light changes through pigment photoprotection (Kudoh et al. 2003, Katayama &Taguchi 2013, Petrou et al. 2016). Therefore, the main objectives of this study were to (1) determine the change in pigment composition including XC pigments related to the photoprotective response of the bottom ice algal community under 2 dominant snow depths (thin and thick) from the beginning of spring to early summer, and (2) investigate the short-term photoacclimation response to an experimental light gradient of bottom ice algae acclimated to 2 snow cover sites.

MATERIALS AND METHODS

Study site, sample collection and experiments

The study was conducted on landfast first-year sea ice, located north of Davis Strait near Qikiqtarjuaq, Nunavut, Canada (67° 28' N, 63° 47' W; Fig. 1), as part of the Green-Edge project. Sea ice samples were collected for measurements of pigments every 2 d from 27 April to 6 July 2015.

For the time series, ice sampling was performed at thick (>25 cm) and thin (15 to 20 cm less than thick snow) snow depths. Snow depth and ice thickness were measured on each ice sampling day with a ruler and an ice thickness gauge (Kovacs Enterprises), respectively. Transmittance of E_{PAR} at the ice–water interface was also measured on each sampling day (see details below). The bottom 3 cm sections were extracted from sea-ice cores using a 14 cm internal diameter ice corer (Mark V Coring System; Kovacs Enterprises). For pigment analysis,

at least 2 ice cores were extracted per snow site and pooled immediately in a dark isothermal container to avoid brine drainage losses. These ice core samples were melted in 0.2 µm filtered seawater (FSW) (3 parts FSW to 1 part melted ice) to minimize osmotic stress on the microbial community during melting (Bates & Cota 1986, Garrison & Buck 1986). Ice–water interface samples for salinity and nutrient determination were collected through an auger hole with a battery-operated plastic submersible pump (Cyclone®) secured to the end of an articulated under-ice arm.

Three distinct types of experiments with ice algae were carried out on 11 occasions between 6 and 31 May 2015 (Table 1). For these experiments, the bottommost 1 cm of 3 sea-ice cores were quickly scraped (McMinn et al. 2005, 2010) and pooled in a dark isothermal container with 0.2 µm FSW (ca. 38 parts FSW to 1 part melted ice) in order to reduce the time of melting, which can impact physiological processes. Indeed, too long of a dark period during the ice melting could result in DT to DD de-epoxidation (Goss & Jakob 2010). In our study, ice samples were melted in less than 30 min. The melted ice was gently mixed, and nutrients were sampled before the water was distributed into clear polycarbonate bottles under dim light conditions (i.e. diffusive light in a Polarhaven shelter with opaque walls and 2 end windows covered by 4 layers of black plastic sheeting).

During the first experiment (Table 1), three 500 ml polycarbonate bottles (E_{PAR} transmittance of ca. 80%) containing ice melt water were placed in each experimental chamber. Each chamber was then exposed to one light intensity (10, 50, 100 or 200 µmol photons m^{-2} s^{-1}) using cool white dimmable LEDS (9 W) and neutral density light filters (LEE Filters). During the experimental period, irradiance at the ice–water interface ranged from 0.3 to 8 µmol photons m^{-2} s^{-1}, and therefore ice algae were acclimated to different light levels in their natural environment. The experimental chambers were continuously cooled with running seawater pumped from the ice–water interface using a small electric submersible pump (Lifegard Aquatics QuietOne Model 1200, 317 GPH). The ice algae were exposed to their respective treatments for 3 h and then placed at the lowest light levels achievable in the field (<5 µmol photons m^{-2} s^{-1}, incubators covered by 4 layers of black plastic sheeting) for a 2 h dark-recovery period. The same experiment was repeated on 7 occasions and the data from the same ice algae (from thin or thick snow) and the same period (before or during snowfall) were averaged. Subsampling for

pulse-amplitude modulation (PAM) fluorometry measurements (i.e. chlorophyll *a* [chl *a*] fluorescence) occurred at 0, 0.5, 1, 2, 3 and 5 h, while pigment composition was assessed at 0, 3 and 5 h.

In the second experiment (Table 1), the relative importance of photoprotection and photorepair mechanisms were assessed using 2 inhibitors: dithiothreitol (DTT) and lincomycin. The xanthophyll inhibitor DTT prevents the de-epoxidation of DD into DT (Olaizola et al. 1994, Lavaud et al. 2002) whereas lincomycin prevents the transcription of chloroplast-encoded D1 proteins (psbA) and therefore inhibits the repair of photodamaged PSII (Petrou et al. 2010). Duplicate 500 ml polycarbonate bottles containing melted ice water from a thin snow cover site were prepared (1) without inhibitor (i.e. control), (2) with DTT (final concentration 100 µmol l^{-1}; Olaizola et al. 1994) and (3) with lincomycin (final concentration 600 µmol l^{-1}; Kropuenske et al. 2009). Approximately 5 min after adding the chemical, the bottles were incubated for 6 h at the ice–water interface using a custom-built under-ice arm. Subsamples for PAM fluorescence and pigment analysis were collected every 2 h between 11:00 and 17:00 h (local time; UTC – 05:00).

In the third experiment (Table 1), duplicate 2 l polycarbonate bottles containing melted ice water from both snow covers were incubated in an opaque-walled incubator located on the snow, exposed to incident irradiance (E_{PAR} + UVR) and continuously cooled with running seawater pumped from the ice–water interface using a small electric submersible pump (Pondmaster magnetic drive utility pump, Model 500 GPH). Subsamples were collected for PAM fluorescence and pigment analysis after 30 min and every hour thereafter for 3 h.

Irradiance measurement

During the study period, transmitted irradiance was measured every sampling day between 10:00 and 11:00 h (local time; UTC – 05:00) using a compact-optical profiling system (C-OPS; Biospherical Instruments). Incident and under-ice downward irradiances were recorded at 19 individual wavelengths (from 320 to 780 nm) by a cosine light sensor. The vertical profile of irradiance under the sea ice was measured by the IcePRO version of the instrument, which is specifically design to fit and sink through a 25 cm diameter ice auger hole. E_{PAR} was computed by constructing a piecewise cubic hermit interpolating polynomial (PCHIP) using downward

irradiance measured at all C-OPS wavelengths and then numerically integrating from 400 to 700 nm to obtain final units of μmol photons m^{-2} s^{-1} (Mobley 1994). The transmitted irradiance at the ice–water interface was calculated as detailed in Belzile et al. (2000). The water column diffuse attenuation coefficient was determined from the linear portion of triplicate measurements of the natural logarithm of the transmitted irradiance versus depth. Due to the alteration of light profiles underneath the ice because of the auger hole and the snow added on it, the E_{PAR} plots were linear, on average, from 10 to 50 m. The r^2 of the relationship between the natural logarithm of the transmitted irradiance versus depth was always >0.99.

To estimate incident irradiance and E_{PAR} at the ice–water interface over a day, we used incident downward shortwave (305 to 2800 nm) radiation, which was measured continuously (as 1 min averages). The shortwave radiation measurements were made using the upward-looking cosine response pyranometer on a 4-sensor net radiometer (Kipp & Zonen; model CNR4) placed at an undisturbed site approximately 20 m west of the meteorological station at a height of 1 m above the snow. The instrument included a heater/ventilator unit (Kipp & Zonen; model CNF4) that cycled on for 5 min at the beginning of every hour to keep the instrument lenses free of snow and frost. We noticed that the heater/ventilator caused a transient increase in measured shortwave radiation under certain atmospheric conditions (light winds, clear skies). In these cases, we used a smoothing algorithm to remove minor data spikes. Incident downward shortwave radiation was converted to E_{PAR} (multiplied by 0.47) as described by Papaioannou et al. (1993). Then the E_{PAR} value in W m^{-2} was converted into μmol photons m^{-2} s^{-1} using a factor of 4.15 as described in Halverson & Pawlowicz (2013). As algae act as scalar collectors with a maximum interception of light incident from all directions due to the arrangement of their photosynthetic tissues, scalar irradiance is the preferred measurement (Kirk 2011). To calculate scalar irradiance at the ice–water interface, we first estimated downward irradiance at the ice–water interface by multiplying the incident downwelling E_{PAR} on the surface by the calculated E_{PAR} transmittance (as detailed above). This subsequent downward irradiance was converted to downward scalar irradiance by dividing by an average cosine factor of 0.7 (Ehn & Mundy 2013). To simplify, we assumed that the upward scalar irradiance was negligible at the ice–water interface. Due to this assumption, we note that our scalar irradiance estimates are likely conservative. Although no direct measurements have been reported, the modeling study of

Pavlov et al. (2017) estimated scalar irradiance at the ice bottom to be ~1.8 times greater than E_{PAR}, in comparison to our estimate that was scaled by a factor of 1.4.

Salinity and nutrients

Salinity of melted ice samples was measured with a hand-held conductivity meter (330i/SET; WTW) calibrated against a 15 N KCl solution at 20°C. Samples for nutrient determination at the ice–water interface and in the experiments were filtered through a pre-combusted (5 h at 450°C) Whatman GF/F glass-fiber filter (nominal porosity of 0.7 µm) inserted in a filter holder. The filtrate was collected into 20 ml polyethylene vials after thorough rinsing. Samples were poisoned with mercuric chloride (final concentration 10 µg ml^{-1}) according to Kirkwood (1992), and stored in the refrigerator until analysis. Nitrate plus nitrite (hereinafter NO_X), nitrite, phosphate and silicic acid were analyzed using a Bran Luebbe Seal autoanalyzer according to the method of Aminot & Kérouel (2007). The analytical detection limits for NO_X, phosphate and silicic acid were 0.05, 0.02 and 0.2 µmol l^{-1}, respectively.

Chl *a* variable fluorescence

To study the photosynthetic responses of algae, PAM fluorometry was used. It is a widely used methodology that provides a rapid, non-invasive assessment of the photosynthetic apparatus of algal cells (Parkhill et al. 2001). It is also a useful tool to examine the ability of photosynthetic organisms to tolerate environmental stressors and the extent of damage caused by these stresses (Maxwell & Johnson 2000). Fluorescence measurements were made with a water-PAM cuvette version with blue LEDs (Walz) inside the unheated field laboratory (Polarhaven shelter), which was set up at the sampling station. All samples were placed in a small cooler containing 2 ice packs during their dark-acclimation for at least 30 min before the measurement of fluorescence. The samples were stirred during measurements.

Minimum (F_0) and maximum fluorescence (F_m) levels were assessed, and the maximum quantum yield of PSII photochemistry (F_v/F_m) was calculated as follows:

$$F_v/F_m = (F_m - F_0) / F_m \quad (1)$$

F_m was obtained using a saturating pulse of ca. 3000 µmol photons m^{-2} s^{-1} for 0.8 s. When measured on a community, F_v/F_m changes must be interpreted with care (see, for example,

Parésys et al. 2005). Nevertheless, in our study, sea-ice algae communities were largely dominated by diatoms (see 'Results'). Hence, F_v/F_m variations can be largely attributed to changes in the photosynthetic efficiency of diatoms.

Rapid light curves (RLCs) were also generated to determine the photosynthetic parameters under both snow covers as a function of snow conditions (before or during snow events). Dark-acclimated samples were exposed to successive increasing actinic light ranging from 0 to 139 µmol photons m^{-2} s^{-1} for 30 s each. The actinic light was measured with a spherical micro quantum sensor US-SQS (Walz). The relative electron transport rate (rETR; dimensionless) values were calculated as follows:

$$rETR = \varphi_{PSII} \times E \quad (2)$$

where $\varphi_{PSII} = (F_m' - F') / F_m'$, known as the operational PSII quantum yield and E is the irradiance applied.

Data from RLCs were fitted using the following equation (Eilers & Peeters 1988, Zonneveld 1998) using a Levenberg-Marquardt regression algorithm:

$$rETR = E / (aE^2 + bE + c) \quad (3)$$

where E is irradiance, and a, b and c are regression coefficients to fit the rETR versus E curve. RLC measurements allow us to describe the main photosynthetic properties of an algal sample, including the maximum ($rETR_{max}$), the light use efficiency (α) represented by the initial slope of the curve (µmol photons m^{-2} $s^{-1})^{-1}$ and the light saturation coefficient (E_k; µmol photons m^{-2} s^{-1}) (Ryan et al. 2009) using the following expressions:

$$\alpha = 1 / c \quad (4)$$

$$rETR_{max} = [b + 2(ac)^{0.5}]^{-1} \quad (5)$$

$$E_k = rETR_{max} / \alpha \quad (6)$$

As for typical ^{14}C P–E curves, these photosynthetic parameters were used to compare the photosynthetic performances and photoacclimation properties of algal communities.

Pigments and CHEMTAX analysis

The identification and concentration of algal pigments were determined by reverse-phase HPLC. Samples (50 to 200 ml, depending on the biomass) were filtered onto 25 mm Whatman GF/F filters using a vacuum pump (0.8 mm Hg), wrapped in aluminum foil and stored immediately at –80°C until analysis. For the time series, the algal pigments of the bottom 3 cm of the ice were extracted at –20°C in 3 ml 100% methanol, disrupted by 10 s of sonication (Bandelin Sonopuls HD2200) and filtered 1 h later through 25 mm Whatman GF/F filters. The pigments were separated and quantified as described in Ras et al. (2008), a method adapted from Van Heukelem & Thomas (2001). Pigments were analyzed using an Agilent Technologies 1200 Series system with a narrow reversed-phase C8 Zorbax Eclipse XDB column (150 × 3 mm, 3.5 µm particle size) which was maintained at 60°C. A diode-array detector allowed measuring the absorption of most pigments at 450 nm, while chl *a* and its derivatives were detected at 667 nm. For the light experiments, the algal pigments were extracted as described in Alou-Font et al. (2013, 2016) and disrupted by 10 s of sonication (Heat Systems; model XL2010). The remaining pigment samples were analyzed using an Agilent Technologies 1200 Series but with a Symmetry C8 column (150 × 4.6 mm, 3.5 µm particle size; Waters Corporation). Pigments were detected with a G1315P diode-array absorbance detector (400 to 700 nm) and chlorophylls were detected by fluorescence (excitation at 400 nm and emission at 650 nm; G1321A fluorescence detector). We used the HPLC separation method described in Zapata et al. (2000). For both methods, pigments were identified based on retention time and spectral properties of external pigment standards, even for degradation pigments (chlorophyllide *a*, pheophytin *a*, pheophorbide *a*) (DHI Lab Products) (Egeland et al. 2011). Limits of detection and quantification were estimated as in Bidigare et al. (2005) and pigments with concentrations below the limit of detection were not reported. In this study, total chl *a* (Tchl *a*) mentioned thereafter corresponds to the sum of chl *a*, chlorophyllide *a*, chl *a* allomer and epimer measured by HPLC. The ratios of photoprotective carotenoids (PPC; including DD, DT, violaxanthin, zeaxanthin and β,β-carotene) to photosynthetic carotenoids (PSC; including fucoxanthin, peridinin, 9'-cis-neoxanthin and alloxanthin) were also calculated. The de-epoxidation state (DES) index, an indicator of photoprotection (Barnett et al. 2015), was expressed as DES = DT / (DD + DT) and calculated for the different experiments.

The contribution of major algal groups to chl *a* was determined from marker pigment ratios using the CHEMical TAXonomy (CHEMTAX) program (Mackey et al. 1996, version 1.95

as used in Wright et al. 2009). According to Mackey et al. (1996), the accuracy of CHEMTAX calculations is optimized when calculations are done on smaller groups of samples, with stable pigment ratios. Thus, samples were separated into 4 data sets with similar environmental (snow depth) and biological (algal bloom phase) conditions. CHEMTAX was used separately on each data set, and the average was calculated for each condition. As the data sets were separated in the same way as those in Alou-Font et al. (2013), we used the same initial pigment ratio matrices defined therein. Therefore, to improve biomass estimation, 10 successive runs of CHEMTAX using the output from each run as the input for the next was used, as recommended by Latasa (2007) and used in recent studies (e.g. Eker-Develi et al. 2012, Liu et al. 2012, Wang et al. 2015). The final ratio matrices are displayed in Table S1 in the Supplement at www.int-res.com/articles/suppl/mXXXpXXX_supp.pdf.

Statistical analysis

Normality of the data was determined using the Shapiro-Wilk test with a 0.05 significance level. When the data were normally distributed, we used parametric tests. For the time series and the third experiment, paired *t*-tests were used to compare paired variables from the thin and thick snow cover sites. For non-parametric data, a Wilcoxon signed rank test was used instead. To determine differences among the 3 sampling periods, a 1-way ANOVA by ranks (Kruskal-Wallis test) was performed and completed by a multiple mean comparison test using rank sums (Dunn's test) adjusted with the Bonferroni method. In addition, Pearson's linear correlations (r) on parametric data were used to infer the relationship between 2 variables. For the first experiment, 1-way repeated ANOVA was performed followed by a post hoc Tukey's test to identify averages that were significantly different between treatments. A *t*-test was also conducted to determine the difference in algal responses (e.g. decline) depending on snow cover. The *t*-statistic, df and p-values are provided in brackets when reported. Statistical tests and graphics were produced with SigmaPlot v.12.3 (Systat Software) and R (R Development Core team 2009).

RESULTS

Change in environmental conditions

Because of temporal changes in snow cover depth resulting from major snow precipitation events on 16 and 20 May, we distinguish 3 sampling periods (i.e. before and during snow events, and snowmelt; Fig. 2). Snow depth remained relatively stable at both sites until 12 May, and increased from ca. 10 to 30 cm and from ca. 25 to 51 cm on 20 May at thin and thick snow cover sites, respectively (Fig. 2a). Thereafter, snow depth slowly decreased at both sites until 9 June, when it decreased faster until reaching 0 cm on 20 June at the thin snow site and later at the thick snow site. Mean sea-ice thickness ranged from 132 to 96 cm during the sampling season (Fig. 2b) and was significantly thinner during the melting period (mean = 116 cm) than during the 2 previous periods (mean = 124 cm) (Dunn's test, $p < 0.05$).

Nutrient concentrations at the ice–water interface varied from 5.38 to 1.38 µmol l^{-1} for NO_X (Fig. 2c), from 0.22 to 0.04 µmol l^{-1} for NO_2^-, from 7.4 to 5.5 µmol l^{-1} for $Si(OH)_4$ and from 0.92 to 0.60 µmol l^{-1} for PO_4^{3-}. NO_X concentrations oscillated between 4.21 and 5.38 µmol l^{-1} from the beginning of the sampling period until 10 June and then started to decrease progressively down to 1.38 µmol l^{-1} at the end of sampling (Fig. 2c). Mean concentrations of NO_X, $Si(OH)_4$ and PO_4^{3-} were significantly lower during the melting period (after 10 June) than during the 2 previous periods (Dunn's test, $p < 0.05$).

E_{PAR} transmittance through the ice and snow remained relatively constant at around 0.06% of incident irradiance until 31 May and then increased progressively up to 4.6% on 6 July due to the complete snowmelt (Fig. 2d). Mean E_{PAR} transmittance was significantly higher after 9 June than before this date (Dunn's test, $p < 0.05$).

Effect of snow events and snow cover depth on ice algal biomass, pigment composition and photosynthetic properties

During the first sampling period (i.e. before snow events), bottom ice Tchl *a* concentration, used as an index of ice algal biomass, was significantly higher under the thin snow (9.28 mg m^{-2}) than under the thick snow (5.14 mg m^{-2}) cover (paired *t*-test, $t = 3.632$, df = 11, $p < 0.01$) (Fig. 3a). During the following 2 periods (i.e. snow events and snowmelt), no significant difference in algal biomass was observed between the 2 snow cover conditions (paired *t*-test, $t = 1.556$, df = 9, $p = 0.15$ during snow events and $t = 0.566$, df = 4, $p = 0.60$ during snowmelt). During the snow events period, bottom ice Tchl *a* concentration reached a

maximum value of 22 mg m^{-2} on 27 May and 32 mg m^{-2} on 2 June at the thick and thin snow sites, respectively. Thereafter, Tchl *a* concentrations decreased progressively to reach a minimum value of 0.18 mg m^{-2} at the thick snow site during the snowmelt period. No samples were collected at the thin snow site after 24 June.

The concentrations of PSC and PPC followed the same trend as Tchl *a*. PSC variations were mainly influenced by fucoxanthin, while PPC were mostly governed by DD and β,β-carotene. The PPC:PSC ratio was relatively constant before and during snow events, with values around 0.1 wt:wt, followed by an increase up to 0.81 wt:wt during the snowmelt period (Fig. 3b). Before snow events, the PPC:PSC ratio was significantly higher under thin snow (0.12 wt:wt) than under thick snow (0.09 wt:wt) (paired *t*-test, $t = 2.393$, $df = 11$, $p < 0.05$). This ratio was positively correlated with E_{PAR} transmittance at the ice–water interface under both thin ($r = 0.816$, $p < 0.001$) and thick snow covers ($r = 0.828$, $p < 0.001$) and during the snowmelt period ($r = 0.812$, $p < 0.001$). Over the entire sampling period, the ratio of (DD+DT) to Tchl *a* followed the same trend as PPC:PSC (Fig. 3b,c). (DD+DT):Tchl *a* was stable around 0.03 wt:wt before and during snow events and increased to 0.28 wt:wt during the snowmelt period under both snow cover conditions. It was significantly higher under thin snow (0.04 wt:wt) than under thick snow (0.02 wt:wt) cover before snow events (paired *t*-test, $t = 3.460$, $df = 11$, $p < 0.01$) and was positively correlated with ice bottom E_{PAR} transmittance during the snowmelt period ($r = 0.667$, $p < 0.05$).

The contributions of major algal groups to chl *a* were determined via CHEMTAX analysis, which showed that diatoms were always dominant under both snow covers during the entire sampling period (>82%; Fig. 4). Diatoms Type 2, containing fucoxanthin and chl c_2 and c_3, were likely associated with pennate diatoms in Alou-Font et al. (2013), while diatoms Type 1 were associated with centric diatoms. Some differences occurred depending on the snow cover and snow periods. Before snow events, diatoms Type 2 (i.e. pennate diatoms) totally dominated under the thin snow cover, while the algal community was more heterogeneous under thick snow with the presence of diatoms Type 1 (16%), cryptophytes (14%) and dinoflagellates (3%). Thereafter, during snow events, the algal community was more heterogeneous under both snow covers, but dinoflagellates (3%) and cryptophytes (2%) were relatively more abundant under thin snow cover. Finally, diatoms entirely dominated the algal community during the snowmelt

period (ca. 99%) with a dominance of diatoms Type 1 (i.e. centric diatoms), but diatoms Type 2 (i.e. pennate diatoms) were 4 times more abundant under thick snow cover (20 vs. 5%). Hence, despite the dominance of diatoms in all samples, some differences in algal community (heterogeneous or diatom types) occurred depending on the environmental conditions.

Before the period of snow events, there was a clear difference in photosynthetic properties and photoacclimation in ice algae living under thin or thick snow cover (Table 2). As expected, α was lower and $rETR_{max}$ was higher under thin snow. As a result, E_k was twice as high (ca. 45 µmol photons m^{-2} s^{-1}) under thin snow. During the snow event period, ice algae under the thin snow cover maintained $rETR_{max}$ and increased α resulting in a E_k decrease of half, reaching a value similar to that under the thick snow cover before the snow event period. Interestingly, ice algae under thick snow cover maintained α (probably because it was already at its maximum), yet increased $rETR_{max}$ to a similar level as ice algae under thin snow cover during snow events.

Effect of a natural range of light exposure on the photophysiology of bottom ice algae as a function of snow conditions

Two types of experiments were performed to determine the short-term effect of enhanced irradiance on the photophysiological response of bottom ice algae (see Table 1). The aim of the first experiment was to assess the short-term effect of enhanced irradiance over a range typically observed at the ice–water interface (10 to 200 µmol photons m^{-2} s^{-1}; see Ryan et al. 2011, Alou-Font et al. 2013) on the photophysiological response of bottom ice algae acclimated to different light environments depending on the snow conditions (i.e. snow depth and snow events). Before snow events, the F_v/F_m ratio, a proxy for the maximum quantum yield for PSII photochemistry, was significantly lower after a 3 h light-exposure to the highest light treatment (i.e. 200 µmol photons m^{-2} s^{-1}) (1-way repeated ANOVAs completed by post hoc Tukey's tests, $q = 4.644$ and $p < 0.05$ for thin snow, and $q = 3.464$ and $p < 0.05$ for thick snow cover) (Fig. 5a,b). The decrease in F_v/F_m was greater for thick snow (t-test, $t = 24$, $p < 0.05$). After 2 h of darkness, F_v/F_m did not change. For the thin snow cover (Fig. 5a), the F_v/F_m response was different with an increase throughout the light exposure and recovery period, especially for the 10 and 50 µmol photons m^{-2} s^{-1} treatments, and it reached final values higher than those at T_0 (ca. 0.55). For

406 thick snow cover (Fig. 5b), F_v/F_m strongly decreased during the first 30 min of illumination in
407 light treatments of 10, 50 and 100 µmol photons m^{-2} s^{-1}, followed by stabilization and a recovery
408 to T_0 values during dark recovery. During snow events (Fig. 5c,d), the F_v/F_m decrease for thin
409 snow cover was significantly different from those before snow events (*t*-test, $t = 3.702$, df = 7, p
410 < 0.01) at 200 µmol photons m^{-2} s^{-1}. F_v/F_m reached the same minima after 3 h of light exposure
411 (ca. 0.30 to 0.35). For lower light intensity treatments, F_v/F_m was rather stable throughout the
412 experiment, except for the 100 µmol photons m^{-2} s^{-1} treatment for thick snow, which showed a
413 stronger decrease and lower recovery than before snow events. Because F_v/F_m is also influenced
414 by nutrient availability *in situ* (Lin et al. 2016) as well as in experimental conditions (Parkhill et
415 al. 2001), we verified that nutrient concentrations were not limiting in our incubation bottles (see
416 Table S2 in the Supplement). Furthermore, due to low primary production (maxima ranged from
417 0.23 to 0.73 µmol C l^{-1} h^{-1}) at the beginning of the experiment (data not shown), dissolved
418 inorganic carbon concentrations (ca. 2105 ± 9.12 µmol kg^{-1}) were sufficient to provide enough
419 carbon for the photosynthesis of ice algae. In addition to F_v/F_m, DES (an index of DD de-
420 epoxidation in bottom ice algae) was assessed (Fig. 6). At T_0, DES varied between 0.05 and 0.09
421 wt:wt and it increased significantly under the 2 highest light treatments (100 and 200 µmol
422 photons m^{-2} s^{-1}) to a maximum level of 0.14 to 0.20 wt:wt. While it was strongly positively
423 correlated with the increase of E_{PAR} at the ice–water interface ($r = 0.85$, $p < 0.001$), no significant
424 difference was observed before or during snow events or between snow covers (thin or thick).
425 After 2 h of dark-recovery, DES decreased back to its T_0 values, independent of snow events and
426 snow depth conditions.

427 In a second, complementary experiment, we aimed to determine the respective
428 importance of DD de-epoxidation and of the synthesis of PSII D1 (psbA) protein to support
429 bottom ice algae in maintaining their photochemical performance when exposed to their natural
430 light environment. For that purpose, bottom ice algae were collected under thin snow cover and
431 incubated at the ice–water interface in the absence (control) and presence of the inhibitor of DD
432 de-epoxidation (i.e. DTT), and of D1 protein synthesis (i.e. lincomycin) (Fig. 7). During the
433 experiment, estimated ice bottom E_{PAR} transmittance progressively decreased from 105 to 53
434 µmol photons m^{-2} s^{-1} from 11:00 to 17:00 h local time (Fig. 7a), a range of irradiance
435 encompassed by that of the first experiment. In all treatments, F_v/F_m decreased during the first 4

h (Fig. 7b; ca. –25 to –30%) until reaching similar values at mid-afternoon (15:00 h) and increased slightly thereafter concomitantly with the sharpest E_{PAR} decrease (from 75 to 53 µmol photons m^{-2} s^{-1}). There was a greater F_v/F_m decline after 2 h light exposure in the presence of DTT and lincomycin (ca. –20 to –25%) in comparison with the control conditions (–5%). It is noteworthy that F_v/F_m response in control conditions after 2 h light exposure was similar to the response observed in our controlled experimental light treatment (Expt 1, thin snow cover, 100 µmol photons m^{-2} s^{-1}; Fig. 5a). In control conditions, DES increased for the first 2 h from 0.063 to 0.086 wt:wt and stabilized until 15:00 h, after which it decreased back to T_0 values, while E_{PAR} at the ice–water interface reached its lowest values (Fig. 7a). In DTT-treated samples, DES was stable around its T_0 value. At T_0, DES in lincomycin-treated samples was significantly higher than in the control and DTT treatments, and did not change during the day, even when E_{PAR} at the ice–water interface decreased. At 17:00 h, F_v/F_m in DTT-treated samples was at 80% of the initial ratio, as for the control, while F_v/F_m in lincomycin-treated samples was only at 40% of the initial ratio. However, DES in lincomycin-treated samples was the highest by a factor of 2 in comparison with other treatments.

Effect of high light exposure on the photophysiology of ice algae released from bottom sea ice

The aim of the third experiment (Table 1) was to assess the photoprotective capability of bottom ice algae when exposed to a sudden increase in irradiance, similar to what they would experience when carried into adjacent ice-free areas by surface currents after their release in the water column. Our hypothesis was that bottom ice algae from thin snow cover should be less light-sensitive than those from thick snow cover. To test this hypothesis, bottom ice algae were collected under thin and thick snow covers and exposed to incident irradiance (Fig. 8). During the experiment, incident E_{PAR} was constant at an average of 1107 ± 95 µmol photons m^{-2} s^{-1} (Fig. 8a).

F_v/F_m of bottom ice algae from thin and thick snow covers reached the same minimum value (ca. 0.05), illustrating a high level of photoinhibition (i.e. –75% in F_v/F_m) when exposed to these over-saturating light intensities (10 times higher than the maximum average of bottom ice; see Fig. 8a) after a 3 h period. Nevertheless, the pattern of F_v/F_m variations was very different

between the 2 algal communities (Fig. 8b). For algae from thin snow cover, F_v/F_m decreased progressively during the first 2 h of light exposure, and sharply during the last hour of exposure. For thick snow cover, F_v/F_m showed a rapid drop close to 0 after the first 0.5 h, followed by a slight but significant recovery to its final value.

At the same time, ice algae underwent substantial changes in pigment content, with a Tchl *a* decrease (Fig. 8c) and DES increase (Fig. 8d); mean values were significantly different under thin and thick snow cover conditions (paired *t*-test, $t = 12.394$, df = 5, $p < 0.001$ for Tchl *a* and Wilcoxon signed rank test, $W = 21$, $p < 0.05$ for DES). More specifically, under thin snow cover, Tchl *a* decreased by 20% (from 1228 to 987 μg chl *a* l^{-1}) during the first 0.5 h of light exposure, followed by a slower but consistent decrease of 23% (from 987 to 759 μg chl *a* l^{-1}) during the rest of the experiment. Simultaneously, DES increased from a value of 0.09 to 0.19 wt:wt during the first 0.5 h of light exposure and then stabilized around a value of 0.18 wt:wt at end of the experiment. Under thick snow cover, Tchl *a* followed a consistent decrease of 33%, from 146 to 98 μg l^{-1} during the 3 h light exposure, while DES did not show significant changes, varying between 0.12 and 0.15 wt:wt.

DISCUSSION

Effect of snow cover on the taxonomic composition and photosynthetic properties of bottom ice algae

According to previous studies at similar latitudes (ca. 70° N) (Renaud et al. 2007, Alou-Font et al. 2013), the ice algal bloom starts between the end of March and beginning of April. In 2015, snow events around mid-May may have extended the ice algal bloom period by reducing E_{PAR} penetration through the ice and thermally insulating the ice, which consequently delayed the melting process that usually terminates the bloom (e.g. Fortier et al. 2002, Mundy et al. 2005, Campbell et al. 2015). Thus, a positive relationship was observed between snow depth and Tchl *a* concentration ($r = 0.693$, $p < 0.001$), contrary to observations for early spring when light is limiting (Mundy et al. 2007, Alou-Font et al. 2013), but consistent with later bloom conditions (Campbell et al. 2015, Leu et al. 2015).

Under both snow covers (thin and thick), the bottom ice algal community was mainly composed of diatoms (Fig. 4), as confirmed by Imaging Flow CytoBot data (P. L. Grondin pers. comm.) and as also reported previously (Alou-Font et al. 2013). Whilst taxonomic studies in the Arctic have shown that pennate diatoms contribute to at least 68% of the abundance of total ice algae (von Quillfeldt et al. 2003, Poulin et al. 2011), we observed a change from a dominance of pennate diatoms (e.g. diatoms Type 2) before snow events to centric diatoms (e.g. diatoms Type 1) during the snowmelt period. This diatom community change from the beginning to the end of spring has recently been observed in Dease Strait (Nunavut) during spring 2014 (Campbell et al. 2017). The transition from pennate to centric diatoms could be associated with the increase in light conditions and changes in physico-chemical properties (e.g. lower brine salinity and limited nutrient availability) of sea ice through the spring season. Furthermore, before snow events (e.g. at the beginning of spring) the algal community under thick snow cover was more heterogeneous, with the presence of cryptophytes and dinoflagellates. This observation was already documented by Różańska et al. (2009) in Franklin Bay, where diatoms were less abundant in sea ice under thick snow than under thin snow. They suggested that flagellates were more abundant due to their capacity to be mixotrophic instead of purely autotrophic (Sherr et al. 2013, Unrein et al. 2014). Thus, the algal composition changed markedly depending on snow cover but also over the different sampling periods.

As the snow melting period progresses, ice algae grow and need to acclimate to higher light intensities. Before snow events, PPC:PSC and (DD+DT):Tchl *a* ratios were higher under thin than thick snow cover conditions (Fig. 3b,c) in accordance with higher light transmittance (Brunelle et al. 2012, Alou-Font et al. 2013). These findings were further corroborated by a lower α, a higher $rETR_{max}$ and a higher E_k under thin snow cover (details in Table 2), a typical high-light acclimation response (McMinn & Hegseth 2004, Manes & Gradinger 2009, Katayama & Taguchi 2013).

During the snowmelt period, bottom ice algae can be exposed for prolonged periods to relatively high light conditions. Thus, they need to be able to protect themselves through, e.g. the synthesis of carotenoids and other antioxidants. The lower bottom ice PPC:PSC ratio (up to 0.81) than previously reported in the Canadian Beaufort Sea (up to 1–3.5 wt:wt; Alou-Font et al. 2013) could be due to the dominance of centric diatoms at the end of spring instead of pennate diatoms.

However, the (DD+DT):Tchl *a* ratio (up to 0.28) was within the range of values reported in the Canadian Beaufort Sea (0.04 to 0.8 wt:wt; Alou-Font et al. 2013), in a high Arctic fjord of Svalbard (0.03 to 0.08 wt:wt; Leu et al. 2010) and in Antarctica (0.08 to 0.1 wt:wt; Petrou et al. 2011, Arrigo 2014). The significant positive relationships between the PPC:PSC and (DD+DT):Tchl *a* ratios and E_{PAR} transmittance at the ice–water interface during the snowmelt period confirms the strong relationship between light transmittance and carotenoids synthesis. By rapid activation of the XC and a rapid decline in photochemical efficiency, bottom ice algae possess a high level of plasticity in their light-acclimation capabilities. Our observations and the previous work of Petrou et al. (2011) in Antarctica confirm that non-photochemical quenching (NPQ) via XC activation would be the preferred method of regulating energy flow to PSII and photoprotection. In addition, the dominance of centric diatoms at the end of spring (Campbell et al. 2017, our Fig. 4) seems to represent the ideal algal community to seed an under-ice bloom. In fact, centric diatoms, as observed with *Chaetoceros* sp. by Petrou & Ralph (2011), possess a high plasticity and are able to acclimate well to all environments, but perform best under pelagic conditions. Thus, in a future Arctic where sea ice will be thinner and consequently light intensities higher, the bottom ice algae could shift from pennate to centric diatoms, based on their differential photoacclimative ability.

Ice algal photophysiological response: the 'cellular light memory' hypothesis

When comparing the photophysiological response of ice algae as a function of snow depth before and during snow events, we observed that ice algae under thick snow cover were more light-sensitive, as indicated by the more rapid decrease of F_v/F_m under light exposure from 10 to 200 µmol photons m^{-2} s^{-1} (Fig. 5). Before snow events, the algal community under thick snow cover was more heterogeneous with the presence of cryptophytes and dinoflagellates, which are more sensitive to greater light intensities than diatoms (Richardson et al. 1983, Demers et al. 1991). Differences in photoacclimative and photoprotective strategies have been reported between diatoms and other algal clades (Rajanahally et al. 2015, Petrou et al. 2016, Lacour et al. 2017) as well as among diatom strains (Lavaud & Goss 2014, Barnett et al. 2015, Petrou et al. 2016). In addition, the lower DES before the experiment (T_0) in this algal community confirmed that it was low-light acclimated before the experiment. Since our experiments were performed under constant temperature (ca. –1.2°C) and nutrient-sufficient conditions, the differences in

552 F_v/F_m and DES between thin and thick snow cover depths could be attributed to the algal
553 community composition and/or the light history of the cells. However, during snow events, the
554 algal community was similar between snow covers, thus the difference in light sensitivity, such
555 as the quicker response of DES and the smaller decrease of F_v/F_m, must be associated with the
556 different light history. The algal community and the light history are then 2 essential factors
557 which must be taken into account when looking at photoprotection and photoacclimation of
558 bottom ice algae.

559 The differential photophysiological response as a function of snow depth was even more
560 pronounced when ice algae were exposed to over-saturating light stress (ca. 1000 µmol photons
561 m^{-2} s^{-1} for 3 h) that mimicked their release from ice and exposure at the surface of open waters.
562 Our experiment confirmed that bottom ice algae from thin snow cover were less light-sensitive
563 than those from thick snow cover. Their light response was supported by their capacity to reduce
564 excitation pressure on PSII (F_v/F_m relatively stable for 2 h) due to a higher DES and synthesis of
565 DT (1.75 times higher than in ice algae from thin snow cover). A similar response was observed
566 in ice algae from Antarctic pack ice (Petrou et al. 2011). Higher DT synthesis illustrates well the
567 response of diatoms to higher average irradiance (Wilhelm et al. 2014) as reported from different
568 algal communities which inhabit substrates and which are dominated by diatoms, i.e. ice algal
569 communities (Arrigo et al. 2010, Petrou et al. 2011, Katayama & Taguchi 2013) as well as
570 benthic diatoms that inhabit intertidal sediments (Laviale et al. 2015). Higher DT cellular content
571 can originate from DD de-epoxidation and de novo synthesis when light conditions are harsher
572 (Lavaud & Goss 2014). Increased DT (and DD) synthesis was recently shown to be directly
573 dependent on the redox state of the plastoquinone (PQ) pool (Lepetit et al. 2013) and thus on the
574 excitation pressure on the photosynthetic machinery, and it is likely related to the parallel
575 synthesis of specific PSII light-harvesting antenna proteins (LHCx; see Wu et al. 2012, Lepetit et
576 al. 2017). Higher DT content provides a stronger capacity to prevent/limit the harmful effects of
577 excess light exposure on photosynthetic efficiency, namely PSII photodamage (Wu et al. 2012,
578 Lepetit et al. 2013) and lipid peroxidation of thylakoid membranes (Lepetit et al. 2010). DT acts
579 via 2 main processes: the dissipation of excess excitation energy in PSII antenna through NPQ
580 (Lavaud & Goss 2014, Goss & Lepetit 2015) and the direct scavenging of reactive oxygen
581 species (ROS) as proposed by Lepetit et al. (2010).

Surprisingly, ice algae under the same snow depth but during different time periods (ca. 25 cm, i.e. thick snow before snow events and thin snow during snow events; Fig. 2a), did not show the same light response (Fig. 5b,c). For all light intensities, the F_v/F_m decrease was stronger for ice algae under thick snow before snow events, indicating a higher light sensitivity. The ice algae under thin snow during snow events showed a similar response to those under thin snow before snow events (Fig. 5a,c) even if they had spent 13 d under the new light conditions (i.e. less light availability because of thicker snow cover) when the experiment took place. This observation suggests that ice algae from thin snow kept their acclimation status similar to that before the snow events, even if they were exposed to lower irradiance (due to snow events) for several days. A similar process, so-called 'cellular light memory', has been reported in higher plants and it can persist for several days (Szechyńska-Hebda et al. 2010, Karpiński & Szechyńska-Hebda 2012). The cellular memory of excess light exposure is based on a complex network in plant tissues which starts in the plastids of leaves, and which orchestrates a physiological response to improve photoacclimation under changing light conditions. It is associated with photoelectrochemical retrograde signaling due in part to changes in PSII redox state, and with photoprotective processes such as the XC-related NPQ. Although diatoms are unicellular organisms, they possess a photoelectrophysiological activity across thylakoid membranes (Bailleul et al. 2015), a redox-based plastid-to-nucleus retrograde signaling pathway (Lepetit et al. 2013) and a strong NPQ tightly associated with the XC (Lavaud & Goss 2014). Based on similar features for photochemistry and light dissipation between higher plants and diatoms, we surmise that diatoms also possess this process of cellular light memory.

Photoprotective mechanisms in low-light acclimated algae

Our study confirms that ice algae were adapted to very low light intensities, but could maintain photosynthesis over a range of irradiances corresponding to those measured at the ice–water interface (up to ca. 100 µmol photons m^{-2} s^{-1}; Fig. 7a). Indeed, fast (within 30 min light exposure) and major changes in PSII photochemistry (decrease in F_v/F_m) and DD de-epoxidation (increased DES) were observed for irradiance of 100 µmol photons m^{-2} s^{-1}. Below this light intensity, the non-significant changes in F_v/F_m and DES indicate that bottom ice algae were acclimated to an irradiance ranging between 50 and 100 µmol photons m^{-2} s^{-1} and probably closer to 50 µmol photons m^{-2} s^{-1} according to our experiments. This observation agrees with the

612 results of Juhl & Krembs (2010), who showed that *Nitzschia frigida* (the most abundant bottom
613 ice pennate diatom in the Arctic) could acclimate up to 110 µmol photons m^{-2} s^{-1} in laboratory
614 conditions. Also similar to our data, Cota & Horne (1989) reported that the optimal
615 photosynthetic irradiance range for ice algae was from 16 to 100 µmol photons m^{-2} s^{-1}. When
616 exposed to 200 µmol photons m^{-2} s^{-1}, and despite the significant increase of DES index, ice
617 algae underwent an important drop down of their photochemistry as indicated by the very low
618 F_v/F_m (ca. 0.3) and its only partial recovery, which well illustrates PSII photoinactivation and/or
619 photodamage (Petrou et al. 2010). This light-response has already been reported for ice algae in
620 Antarctica (Petrou et al. 2010, 2011). In contrast, studies in Greenland and Antarctica found that
621 highly shade-adapted ice diatoms showed a photoinhibitory response at irradiances as low as 25
622 to 50 µmol photons m^{-2} s^{-1} (e.g. Rysgaard et al. 2001, McMinn et al. 2007, Mangoni et al. 2009,
623 Ryan et al. 2011). Nutrient availability (Cota & Horne 1989) could well explain this discrepancy
624 with our data as well as differential photoadaptation abilities among diatom species and
625 communities between our data and others (Laviale et al. 2015, Petrou et al. 2016). Thus,
626 environmental (e.g. nutrient concentrations and light conditions depending on snow depth) and
627 biological (e.g. algal community composition) conditions influence the photo-response of ice
628 algae, which can acclimate to a range of irradiances from 25 up to 100 µmol photons m^{-2} s^{-1}
629 according to the literature and this study. It is noteworthy that ice algae could be more light
630 resistant when aggregated (a behavioral feature we could not assess with the design of our
631 experiments). In fact, aggregation of ice algae during spring and generated self-shading are 2
632 processes often mentioned in Arctic studies (Glud et al. 2002, Assmy et al. 2013, Fernández-
633 Méndez et al. 2014), and it could expand their range of light resistance beyond 100 µmol
634 photons m^{-2} s^{-1}.

635 In order to better understand the photophysiological response of ice algae, we compared
636 the effects of presence and absence of an inhibitor of de-epoxidation of DD into DT (i.e. DTT)
637 and of PSII photodamage repair (i.e. lincomycin). This single experiment with duplicate samples
638 gives us an idea of the relative importance of DT and PSII D1 protein synthesis in
639 photoprotection and in the maintenance of photosynthesis under an irradiance range (ca. 50 to
640 100 µmol photons m^{-2} s^{-1}) that ice algae experience at the ice–water interface (Fig. 7a).
641 Although this type of experiment has been previously conducted (DTT: Kudoh et al. 2003,

642 Griffith et al. 2009; lincomycin: Petrou et al. 2010), this was the first time that such a combined
643 protocol was applied on an Arctic ice algal community. As during our controlled experiments,
644 bottom ice algae were able to maintain their photosynthetic capacity (mostly high and stable
645 F_v/F_m) under these light conditions. Differential light-response between control conditions and
646 inhibitor treatments indicate that PSII photochemical functionality was supported by both DT
647 and D1-psbA protein synthesis with an apparently stronger photoprotective capacity by DT
648 synthesized from DD de-epoxidation (i.e. F_v/F_m decrease was significantly higher when DTT
649 was added as compared to lincomycin). This is in agreement with previous reports on Antarctic
650 bottom ice algae, showing that they are well adapted to their changing *in situ* light environment
651 as indicated by no/low PSII photodamage due to DT and D1-psbA protein synthesis (Petrou et al.
652 2010, 2011). However, when ice algae were exposed to an over-saturating light stress (ca. 1000
653 µmol photons m^{-2} s^{-1}), their photochemical capacity was nearly abolished after 3 h, although
654 efficient DT-driven photoprotection occurred during the first 2 h. This response could be
655 associated with high E_{PAR} but also with the presence of UVR in this experiment, while it was
656 absent in the others. Some studies showed that pennate diatoms were relatively tolerant of UVR
657 (Zacher et al. 2007, Wulff et al. 2008), while a recent study on ice algal communities in the
658 Baltic Sea observed that UVR was one of the controlling factors (Enberg et al. 2015). In
659 addition, studies on Antarctic algal cultures exposed to UVR observed an increase in mortality
660 (McMinn et al. 1999), a reduction in photosynthesis (Schoeld et al. 1995, Villafañe et al. 2004)
661 and a decline in productivity (Marcoval et al. 2007). Such light conditions can occur when ice
662 algae released from sea ice are exported towards the surface of open waters along a receding ice
663 edge. Our observation strongly points to the inability of ice algae to manage with a high rate of
664 PSII photodamage generating photoinhibition. However, as mentioned above, they can also
665 protect themselves via self-shading by forming aggregates when released into the water column
666 (Glud et al. 2002, Assmy et al. 2013, Fernández-Méndez et al. 2014). This process enhances the
667 sinking rate of sea ice algae, especially of diatoms (Raven & Waite 2004, Aumack & Juhl 2015),
668 and their export to deeper water layers where they can feed both pelagic and benthic food webs
669 (Kohlbach et al. 2016).

670 **CONCLUSIONS**

In this study, bottom ice algae were dominated by diatoms and were well adapted to daily and weekly changes in their light environment during Arctic spring. This is in agreement with previous studies in Antarctica (e.g. McMinn et al. 2007, Mangoni et al. 2009, Petrou et al. 2011, Rajanahally et al. 2015). Their rapid response to excess light exposure is supported by central photoprotective processes such as XC and the repair of photodamaged D1 protein in PSII. We found that the photoprotective ability of bottom ice algae depends on their light history, controlled by the overlying snow depth through its influence on light transmittance to the bottom ice environment. We propose that, in order to acclimate to their permanently changing light environment driven by snow events and winds, bottom ice algae perform 'cellular light memory' similar to higher plants (Szechyńska-Hebda et al. 2010). According to our data, cellular light memory can prolong over at least 2 wk, enabling ice algae to improve their photoacclimative response to changing light conditions over different periods (days vs. weeks).

In a context of global warming in the Arctic, it has been predicted that the snow cover will potentially undergo rapid changes during future Arctic spring due to the combined effects of an increase in snow events (Singarayer et al. 2006, AMAP 2011) yet a decrease in snow depth (Webster et al. 2014) and duration (Callaghan et al. 2011, Derksen & Brown 2012, Overland et al. 2014). This will directly and strongly affect the light availability for bottom ice algae. The high plasticity of ice algae to acclimate to relatively large variations in irradiance over very different time scales suggests that ice algae may be more resilient to future changes than previously anticipated. However, ice algae will likely face more frequent light stress due to disturbed sea ice dynamics and especially an earlier melt (Leu et al. 2016). As shown in our study, bottom ice algae can only sustain reversible photoinhibition under high-light conditions for a limited period (less than 3 h), greatly reducing their productivity and survival potential once released into the water column at the ice edge (Yamamoto et al. 2014). In this context, the timing between snowmelt, the release of ice algae and their stage of development will certainly affect their photoacclimative and photoprotective responses. Thus, it would be of interest to achieve similar light-response experiments on bottom ice algae during the decline of their spring bloom and the beginning of their release from sea ice.

Acknowledgements. We acknowledge the contributions of the Canada Excellence Research Chair (CERC) and Canada Research Chair (CRC) programs, the Natural Sciences and Engineering Research Council of Canada (NSERC), the Canada Foundation for Innovation (CFI), Canada

Economic Development, and Fonds de recherche du Québec – Nature et technologies (FRQNT) through the Québec-Océan research cluster. The GreenEdge project is funded by the following French and Canadian programs and agencies: ANR (Contract #111112), CNES (project #131425), IPEV (project #1164), CSA, Fondation Total, ArcticNet, LEFE, and the French Arctic Initiative (GreenEdge project). This project would not have been possible without the support of the Hamlet of Qikiqtarjuaq and the members of the community as well as the Inuksuit School and its Principal J. Arsenault. The project was conducted under the scientific coordination of the Canada Excellence Research Chair on Remote sensing of Canada's new Arctic frontier and the CNRS & Université Laval Takuvik Joint International laboratory (UMI3376). The field campaign was successful thanks to the contribution of J. Ferland, G. Bécu, C. Marec, J. Lagunas, F. Bruyant, J. Larivière, E. Rehm, S. Lambert-Girard, C. Aubry, C. Lalande, A. LeBaron, C. Marty, J. Sansoulet, D. Christiansen-Stowe, A. Wells, M. Benoît-Gagné, E. Devred and M.-H. Forget from the Takuvik laboratory, as well as F. Pinczon du Sel and E. Brossier from Vagabond. We also thank the CCGS 'Amundsen' and the Polar Continental Shelf Program for their in-kind contribution in polar logistic and scientific equipment. The authors thank M. Blais, J. Charette and M. Simard for their invaluable help with the analysis and identification of pigments. We also thank the participants of the Green Edge ice camp for their precious help during the experiments and G. Neukermans for achieving C-OPS profiles. We are grateful to P. Raimbaud (UMR 6117 CNRS) for the nutrient analysis and H. Claustre, J. Ras and C. Dimier (SAPIGH-Villefranche Oceanographic Laboratory) for HPLC analysis. We thank G. Joyal (P. Lajeunesse laboratory from Laval University) who provided the bathymetric data for the map. The authors are grateful to 3 anonymous reviewers whose constructive comments greatly improved the quality of the manuscript. This is a contribution to the research programs of ArcticNet, Québec-Océan, Arctic Science Partnership (ASP) and the Canada Excellence Research Chair unit at the Centre for Earth Observation Science.

LITERATURE CITED

Alou-Font E, Mundy CJ, Roy S, Gosselin M, Agustí S (2013) Snow cover affects ice algal pigment composition in the coastal Arctic Ocean during spring. Mar Ecol Prog Ser 474:89–104 https://doi.org/10.3354/meps10107

731 Alou-Font E, Roy S, Agustí S, Gosselin M (2016) Cell viability, pigments and photosynthetic
732 performance of Arctic phytoplankton in contrasting ice-covered and open-water conditions
733 during the spring-summer transition. Mar Ecol Prog Ser 543:89–106
734 https://doi.org/10.3354/meps11562

735 AMAP (2011) Snow, water, ice and permafrost in the Arctic (SWIPA): climate change and the
736 cryosphere. Arctic monitoring and assessment programme (AMAP), Oslo

737 Aminot A, Kérouel R (2007) Dosage automatique des nutriments dans les eaux marines:
738 méthodes en flux continu. Edition Quae, Versailles

739 Arrigo KR (2014) Sea ice ecosystems. Annu Rev Mar Sci 6:439–467 https://doi.org/10.1146/annurev-
740 marine-010213-135103

741 Arrigo KR, Sullivan CW (1992) The influence of salinity and temperature covariation on the
742 photophysiological characteristics of Antarctic sea ice microalgae. J Phycol 28:746–756
743 https://doi.org/10.1111/j.0022-3646.1992.00746.x

744 Arrigo KR, Kremer JN, Sullivan CW (1993) A simulated Antarctic fast-ice ecosystem. J
745 Geophys Res 98:6929–6946 https://doi.org/10.1029/93JC00141

746 Arrigo K, Mock T, Lizotte MP (2010) Primary producers and sea ice. In: Thomas DN,
747 Dieckmann GS (eds) Sea ice. Wiley-Blackwell, West Sussex, p 283–325

748 Assmy P, Ehn JK, Fernández-Méndez M, Hop H and others (2013) Floating ice-algal aggregates
749 below melting Arctic sea ice. PLOS ONE 8:e76599 https://doi.org/10.1371/journal.pone.0076599

750 Aumack CF, Juhl AR (2015) Light and nutrient effects on the settling characteristics of the sea
751 ice diatom *Nitzschia frigida*. Limnol Oceanogr 60:765–776
752 https://doi.org/10.1002/lno.10054Aumack CF, Juhl AR, Krembs C (2014) Diatom vertical
753 migration within land-fast Arctic sea ice. J Mar Syst 139:496–504
754 https://doi.org/10.1016/j.jmarsys.2014.08.013

755 Bailleul B, Berne N, Murik O, Petrousos D and others (2015) Energetic coupling between
756 plastids and mitochondria drives CO_2 assimilation in diatoms. Nature 524:366–369
757 https://doi.org/10.1038/nature14599

Ban A, Aikawa S, Hattori H, Sasaki H and others (2006) Comparative analysis of photosynthetic properties in ice algae and phytoplankton inhabiting Franklin Bay, the Canadian Arctic, with those in mesophilic diatoms during CASES 03–04. Polar Biosci 19:11–28

Barlow RG, Gosselin M, Legendre L, Therriault JC, Demers S, Llewellyn A, Mantoura RFC (1988) Photoadaptive strategies in sea-ice microalgae. Mar Ecol Prog Ser 45:145–152 https://doi.org/10.3354/meps045145

Barnett A, Méléder V, Blommaert L, Lepetit B and others (2015) Growth form defines physiological photoprotective capacity in intertidal benthic diatoms. ISME J 9:32–45 https://doi.org/10.1038/ismej.2014.105

Bates SS, Cota FC (1986) Fluorescence induction and photosynthetic responses of Arctic ice algae to sample treatment and salinity. J Phycol 70:421–429 https://doi.org/10.1111/j.1529-8817.1986.tb02484.xBelzile C, Johannessen SC, Gosselin M, Demers S, Miller WL (2000) Ultraviolet attenuation by dissolved and particulate constituents of first-year ice during late spring in an Arctic polynya. Limnol Oceanogr 45:1265–1273 https://doi.org/10.4319/lo.2000.45.6.1265

Bidigare RR, Van Heukelem L, Trees CC (2005) Analysis of algal pigments by high-performance liquid chromatography. In: Andersen RA (ed) Algal culturing techniques. Elsevier Academic Press, Burlington, MA, p 327–346

Brunelle CB, Larouche P, Gosselin M (2012) Variability of phytoplankton light absorption in Canadian Arctic seas. J Geophys Res 117:C00G17 https://doi.org/10.1029/2011JC007345

<edb>Brunet C, Johnsen G, Lavaud J, Roy S (2011) Pigments and photoacclimation processes. In: Roy S, Llewellyn CA, Egeland ES, Johnsen G (eds) Phytoplankton pigments: characterization, chemotaxonomy and applications in oceanography. Cambridge University Press, Cambridge, p 445–454</edb>

<jrn>Callaghan TV, Johansson M, Brown RD, Groisman PY and others (2011) Multiple effects of changes in Arctic snow cover. Ambio 40:32–45 doi:10.1007/s13280-011-0213-x</jrn>

<jrn>Campbell K, Mundy CJ, Barber D, Gosselin M (2014) Remote estimates of ice algae biomass and their response to environmental conditions during spring melt. Arctic 67:375–387 doi:10.14430/arctic4409</jrn>

<jrn>Campbell K, Mundy CJ, Barber D, Gosselin M (2015) Characterizing the sea ice algae chlorophyll *a* snow depth relationship over Arctic spring melt using transmitted irradiance. J Mar Syst 147:76–84 doi:10.1016/j.jmarsys.2014.01.008</jrn>

<unknown>Campbell K, Mundy CJ, Belzile C, Delaforge A, Rysgaard S (2017) Seasonal dynamics of algal and bacterial communities in Arctic sea ice under variable snow cover. Polar Biol, doi:10.1007/s00300-017-2168-2</unknown>

<jrn>Comiso JC, Hall DK (2014) Climate trends in the Arctic as observed from space. Wiley Interdiscip Rev Clim Change 5:389–409 PubMed doi:10.1002/wcc.277</jrn>

<jrn>Cota GF (1985) Photoadaptation of high Arctic ice algae. Nature 315:219–222 doi:10.1038/315219a0</jrn>

<jrn>Cota GF, Horne EPW (1989) Physical control of Arctic ice algal production. Mar Ecol Prog Ser 52:111–121 doi:10.3354/meps052111</jrn>

<jrn>Demers S, Roy S, Gagnon R, Vignault C (1991) Rapid light-induced changes in cell fluorescence and in xanthophyll-cycle pigments of *Alexandrium excavatum* (Dinophyceae) and *Thalassiosira pseudonana* (Bacillariophyceae): a photo-protection mechanism. Mar Ecol Prog Ser 76:185–193 doi:10.3354/meps076185</jrn>

<jrn>Derksen C, Brown R (2012) Spring snow cover extent reductions in the 2008–2012 period exceeding climate model projections. Geophys Res Lett 39:L19504 doi:10.1029/2012GL053387</jrn>

<edb>Egeland ES, Garrido JL, Clementson L, Andresen K and others (2011) Data sheets aiding identification of phytoplankton carotenoids and chlorophylls. In: Roy S, Llewellyn CA, Egeland ES, Johnsen G (eds) Phytoplankton pigments: characterization, chemotaxonomy and applications in oceanography. Cambridge University Press, Cambridge, p 665–822</edb>

<jrn>Ehn JK, Mundy CJ (2013) Assessment of light absorption within highly scattering bottom sea ice from under-ice light measurements: implications for Arctic ice algae primary production. Limnol Oceanogr 58:893–902 doi:10.4319/lo.2013.58.3.0893</jrn>

<jrn>Eilers PHC, Peeters JCH (1988) A model for the relationship between light intensity and the rate of photosynthesis in phytoplankton. Ecol Modell 42:199–215 doi:10.1016/0304-3800(88)90057-9</jrn>

816 <jrn>Eker-Develi E, Berthon JF, Canuti E, Slabakova N, Moncheva S, Shtereva G, Dzhurova B
817 (2012) Phytoplankton taxonomy based on CHEMTAX and microscopy in the northwestern
818 Black Sea. J Mar Syst 94:18–32 doi:10.1016/j.jmarsys.2011.10.005</jrn>

819 <jrn>Enberg S, Piiparinen J, Majaneva M, Vähätalo AV, Autio R, Rintala JM (2015) Solar PAR
820 and UVR modify the community composition and photosynthetic activity of sea ice algae.
821 FEMS Microbiol Ecol 91:fiv102 PubMed doi:10.1093/femsec/fiv102</jrn>

822 <jrn>Fernández-Méndez M, Wenzhöfer F, Peeken I, Sørensen HL, Glud RN, Boetius A (2014)
823 Composition, buoyancy regulation and fate of ice algal aggregates in the central Arctic
824 Ocean. PLOS ONE 9:e107452 PubMed doi:10.1371/journal.pone.0107452</jrn>

825 <jrn>Garrison DL, Buck KR (1986) Organism losses during ice melting: a serious bias in sea ice
826 community studies. Polar Biol 6:237–239 doi:10.1007/BF00443401</jrn>

827 <jrn>Glud RN, Rysgaard S, Kühl M (2002) A laboratory study on O_2 dynamics and
828 photosynthesis in ice algal communities: quantification by microsensors, O_2 exchange
829 rates,^{14}C incubations and a PAM fluorometer. Aquat Microb Ecol 27:301–311
830 doi:10.3354/ame027301</jrn>

831 <jrn>Goss R, Jakob T (2010) Regulation and function of xanthophyll cycle-dependent
832 photoprotection in algae. Photosynth Res 106:103–122 PubMed doi:10.1007/s11120-010-
833 9536-x</jrn>

834 <jrn>Goss R, Lepetit B (2015) Biodiversity of NPQ. J Plant Physiol 172:13–32 PubMed
835 doi:10.1016/j.jplph.2014.03.004</jrn>

836 <jrn>Gosselin M, Legendre L, Demers S, Ingram RG (1985) Responses of sea-ice microalgae to
837 climatic and fortnightly tidal energy inputs (Manitounuk Sound, Hudson Bay). Can J Fish
838 Aquat Sci 42:999–1006 doi:10.1139/f85-125</jrn>

839 <jrn>Gosselin M, Levasseur M, Wheeler P, Horner RA, Booth B (1997) New measurements of
840 phytoplankton and ice algal production in the Arctic Ocean. Deep Sea Res II 44:1623–1644
841 doi:10.1016/S0967-0645(97)00054-4</jrn>

842 <jrn>Griffith GP, Vennell R, Lamare MD (2009) Diadinoxanthin cycle of the bottom ice algal
843 community during spring in McMurdo Sound, Antarctica. Polar Biol 32:623–636
844 doi:10.1007/s00300-008-0562-5</jrn>

845 <jrn>Ha SY, Lee DB, Kang SH, Shin KH (2016) Strategy of photo-protection in phytoplankton
846 assemblages in the Kongsfjorden, Svalbard, Arctic. Chin J Oceanology Limnol 34:1–12
847 doi:10.1007/s00343-015-4295-3</jrn>

848 <jrn>Halverson MJ, Pawlowicz R (2013) High-resolution observations of chlorophyll-a biomass
849 from an instrumented ferry: influence of the Fraser River plume from 2003 to 2006. Cont
850 Shelf Res 59:52–64 doi:10.1016/j.csr.2013.04.010</jrn>

851 <jrn>Johnsen G, Hegseth EN (1991) Photoadaptation of sea-ice microalgae in the Barents Sea.
852 Polar Biol 11:179–184 doi:10.1007/BF00240206</jrn>

853 <jrn>Juhl AR, Krembs C (2010) Effects of snow removal and algal photoacclimation on growth
854 and export of ice algae. Polar Biol 33:1057–1065 doi:10.1007/s00300-010-0784-1</jrn>

855 <jrn>Juhl AR, Krembs C, Meiners KM (2011) Seasonal development and differential retention
856 of ice algae and other organic fractions in first-year Arctic sea ice. Mar Ecol Prog Ser 436:1–
857 16 doi:10.3354/meps09277</jrn>

858 <jrn>Karpiński S, Szechyńska-Hebda M (2012) Cellular light memory, photo-electrochemical
859 and redox retrograde signaling in plants. BioTechnologia 93:27–39
860 doi:10.5114/bta.2012.46566</jrn>

861 <jrn>Kashino Y, Kudoh S, Hayashi Y, Suzuki Y and others (2002) Strategies of phytoplankton
862 to perform effective photosynthesis in the North Water. Deep Sea Res II 49:5049–5061
863 doi:10.1016/S0967-0645(02)00177-7</jrn>

864 <jrn>Katayama T, Taguchi S (2013) Photoprotective responses of an ice algal community in
865 Saroma-Ko Lagoon, Hokkaido, Japan. Polar Biol 36:1431–1439 doi:10.1007/s00300-013-
866 1361-1</jrn>

867 <jrn>Katayama T, Makabe R, Sampei M, Hattori H, Sasaki H, Taguchi S (2017) Photoprotection
868 and recovery of photosystem II in the Southern Ocean phytoplankton. Polar Sci 12:5–11
869 doi:10.1016/j.polar.2016.12.003</jrn>

870 <edb>Kirk JTO (2011) Scalar irradiance. In: Light and photosynthesis in aquatic ecosystems, 3rd
871 edn. Cambridge University Press, Cambridge, p 143</edb>

872 <jrn>Kirkwood DS (1992) Stability of solutions of nutrient salts during storage. Mar Chem
873 38:151–164 doi:10.1016/0304-4203(92)90032-6</jrn>

874 <jrn>Kohlbach D, Graeve M, Lange BA, David C, Peeken I, Flores H (2016) The importance of
875 ice algae-produced carbon in the central Arctic Ocean ecosystem: food web relationships
876 revealed by lipid and stable isotope analyses. Limnol Oceanogr 61:2027–2044
877 doi:10.1002/lno.10351</jrn>

878 <jrn>Kropuenske LR, Mills MM, van Dijken GL, Bialey S, Robinson DH, Welschmeyer NA,
879 Arrigo KR (2009) Photophysiology in two major Southern Ocean phytoplankton taxa:
880 photoprotection in *Phaeocystis antarctica* and *Fragilariopsis cylindrus*. Limnol Oceanogr
881 54:1176–1196 doi:10.4319/lo.2009.54.4.1176</jrn>

882 <jrn>Kuczynska P, Jemiola-Rzeminska M, Strzalka K (2015) Photosynthetic pigments in
883 diatoms. Mar Drugs 13:5847–5881 PubMed doi:10.3390/md13095847</jrn>

884 <jrn>Kudoh S, Robineau B, Suzuki Y, Fujiyoshi Y, Takahashi M (1997) Photosynthetic
885 acclimation and the estimation of temperate ice algal primary production in Saroma-ko
886 Lagoon, Japan. J Mar Syst 11:93–109 doi:10.1016/S0924-7963(96)00031-0</jrn>

887 <jrn>Kudoh S, Imura S, Kashino Y (2003) Xanthophyll-cycle of ice algae on the sea ice bottom
888 in Saroma Ko lagoon, Hokkaido, Japan. Polar Biosci 16:86–97</jrn>

889 <jrn>Kühl M, Glud RN, Borum J, Roberts R, Rysgaard S (2001) Photosynthetic performance of
890 surface-associated algae below sea ice as measured with pulse amplitude modulated (PAM)
891 fluorometer and O_2 microsensors. Mar Ecol Prog Ser 223:1–14
892 doi:10.3354/meps223001</jrn>

893 <jrn>Lacour T, Larivière J, Babin M (2017) Growth, chl *a* content, photosynthesis, and
894 elemental composition in polar and temperate microalgae. Limnol Oceanogr 62:43–58
895 doi:10.1002/lno.10369</jrn>

896 <jrn>Latasa M (2007) Improving estimations of phytoplankton class abundances using
897 CHEMTAX. Mar Ecol Prog Ser 329:13–21 doi:10.3354/meps329013</jrn>

898 <edb>Lavaud J, Goss R (2014) The peculiar features of non-photochemical fluorescence
899 quenching in diatoms and brown algae. In: Demming-Adams B, Garab G, Adams W III,

Govindjee (eds) Non-photochemical quenching and energy dissipation in plants, algae and cyanobacteria. Springer, Dordrecht, p 421–443, doi:10.1007/978-94-017-9032-1</edb>

<jrn>Lavaud J, Rousseau B, van Gorkom H, Etienne AL (2002) Influence of the diadinoxanthin pool size on photoprotection in the marine planktonic diatom *Phaeodactylum tricornutum*. Plant Physiol 129:1398–1406 PubMed doi:10.1104/pp.002014</jrn>

<jrn>Laviale M, Barnett A, Ezequiel J, Lepetit B and others (2015) Response of intertidal benthic microalgal biofilms to a coupled light–temperature stress: evidence for latitudinal adaptation along the Atlantic coast of southern Europe. Environ Microbiol 17:3662–3677 PubMed doi:10.1111/1462-2920.12728</jrn>

<jrn>Lavoie D, Denman KL, Michel C (2005) Modeling ice algal growth and decline in a seasonally ice-covered region of the Arctic (Resolute Passage, Canadian Archipelago). J Geophys Res 110:C11009 doi:10.1029/2005JC002922</jrn>

<jrn>Lazzara L, Nardello I, Gallo C, Mangoni O, Saggiomo V (2007) Light environment and seasonal dynamics of microalgae in the annual sea ice at Terra Nova Bay (Ross Sea, Antarctica). Antarct Sci 19:83–92 doi:10.1017/S0954102007000119</jrn>

<jrn>Legendre L, Ackley S, Dieckmann G, Gulliksen B and others (1992) Ecology of sea ice biota. Polar Biol 12:429–444</jrn>

<jrn>Lepetit B, Volke D, Gilbert M, Wilhelm C, Goss R (2010) Evidence for the existence of one antenna-associated, lipid-dissolved and two protein-bound pools of diadinoxanthin cycle pigments in diatoms. Plant Physiol 154:1905–1920 PubMed doi:10.1104/pp.110.166454</jrn>

<jrn>Lepetit B, Sturm S, Rogato A, Gruber A and others (2013) High light acclimation in the secondary plastids containing diatom *Phaeodactylum tricornutum* is triggered by the redox state of the plastoquinone pool. Plant Physiol 161:853–865 PubMed doi:10.1104/pp.112.207811</jrn>

<jrn>Lepetit B, Gélin G, Lepetit M, Sturm S and others (2017) The diatom *Phaeodactylum tricornutum* adjusts nonphotochemical fluorescence quenching capacity in response to dynamic light via fine-tuned Lhcx and xanthophyll cycle pigment synthesis. New Phytol 214:205–218 PubMed doi:10.1111/nph.14337</jrn>

<jrn>Leu E, Wiktor J, Søreide JE, Berge J, Falk-Petersen S (2010) Increased irradiance reduces food quality of sea ice algae. Mar Ecol Prog Ser 411:49–60 doi:10.3354/meps08647</jrn>

<jrn>Leu E, Mundy CJ, Assmy P, Campbell K and others (2015) Arctic spring awakening – steering principles behind the phenology of vernal ice algae blooms. Prog Oceanogr 139:151–170 doi:10.1016/j.pocean.2015.07.012</jrn>

<jrn>Leu E, Graeve M, Wulff A (2016) A (too) bright future? Arctic diatoms under radiation stress. Polar Biol 39:1711–1724 doi:10.1007/s00300-016-2003-1</jrn>

<jrn>Lin H, Kuzminov FI, Park J, Lee SH, Falkowski PG, Gorbunov MY (2016) The fate of photons absorbed by phytoplankton in the global ocean. Science 351:264–267 PubMed doi:10.1126/science.aab2213</jrn>

<jrn>Liu X, Huang B, Liu Z, Wang L, Wei H, Li C, Huang Q (2012) High-resolution phytoplankton diel variations in the summer stratified central Yellow Sea. J Oceanogr 68:913–927 doi:10.1007/s10872-012-0144-6</jrn>

<jrn>Lizotte MP, Sullivan CW (1992) Photosynthetic capacity in microalgae associated with Antarctic pack ice. Polar Biol 12:497–502 doi:10.1007/BF00238188</jrn>

<jrn>Loose B, Miller LA, Elliott S, Papakyriakou T (2011) Sea ice biogeochemistry and material transport across the frozen interface. Oceanography (Wash DC) 24:202–218 doi:10.5670/oceanog.2011.72</jrn>

<jrn>Lund-Hansen LC, Hawes I, Sorrell BK, Nielsen MH (2014) Removal of snow cover inhibits spring growth of Arctic ice algae through physiological and behavioral effects. Polar Biol 37:471–481 doi:10.1007/s00300-013-1444-z</jrn>

<jrn>Mackey MD, Mackey DJ, Higgins HW, Wright SW (1996) CHEMTAX— a program for estimating class abundances from chemical markers: application to HPLC measurements of phytoplankton. Mar Ecol Prog Ser 144:265–283 doi:10.3354/meps144265</jrn>

<jrn>Malviya S, Scalco E, Audic S, Vincent F and others (2016) Insights into global diatom distribution and diversity in the world's ocean. Proc Natl Acad Sci USA 113:E1516–E1525 PubMed doi:10.1073/pnas.1509523113</jrn>

<jrn>Manes SS, Gradinger R (2009) Small scale vertical gradients of Arctic ice algal photophysiological properties. Photosynth Res 102:53–66 PubMed doi:10.1007/s11120-009-9489-0</jrn>

<jrn>Mangoni O, Carrada GC, Modigh M, Catalano G, Saggiomo V (2009) Photoacclimation in Antarctic bottom ice algae: an experimental approach. Polar Biol 32:325–335 doi:10.1007/s00300-008-0517-x</jrn>

<jrn>Markus T, Stroeve JC, Miller J (2009) Recent changes in Arctic sea ice melt onset, freeze up, and melt season length. J Geophys Res Oceans 114:C12024 doi:10.1029/2009JC005436</jrn>

<jrn>Maxwell K, Johnson GN (2000) Chlorophyll fluorescence—a practical guide. J Exp Bot 51:659–668 PubMed doi:10.1093/jexbot/51.345.659</jrn>

<jrn>McMinn A, Hegseth EN (2004) Quantum yield and photosynthetic parameters of marine microalgae from the southern Arctic Ocean, Svalbard. J Mar Biol Assoc UK 84:865–871 doi:10.1017/S0025315404010112h</jrn>

<jrn>McMinn A, Hirawake T, Hamaoka T, Hattori H, Fukuchi M (2005) Contribution of benthic microalgae to ice covered coastal ecosystems in northern Hokkaido, Japan. J Mar Biol Assoc UK 85:283–289 doi:10.1017/S002531540501173h</jrn>

<jrn>McMinn A, Ryan KG, Ralph PJ, Pankowski A (2007) Spring sea-ice photosynthesis, primary productivity and biomass distribution in eastern Antarctica, 2002–2004. Mar Biol 151:985–995 doi:10.1007/s00227-006-0533-8</jrn>

<jrn>McMinn A, Martin A, Ryan K (2010) Phytoplankton and sea ice algal biomass and physiology during the transition between winter and spring (McMurdo Sound, Antarctica). Polar Biol 33:1547–1556 doi:10.1007/s00300-010-0844-6</jrn>

<jrn>Michel C, Legendre L, Demers S, Therriault JC (1988) Photo-adaptation of sea-ice microalgae in springtime: photosynthesis and carboxylating enzymes. Mar Ecol Prog Ser 50:177–185 doi:10.3354/meps050177</jrn>

<jrn>Michel C, Ingram RG, Harris LR (2006) Variability in oceanographic and ecological processes in the Canadian Arctic Archipelago. Prog Oceanogr 71:379–401 doi:10.1016/j.pocean.2006.09.006</jrn>

985 <bok>Mobley CD (1994) Light and water radiative transfer in natural waters. Academic Press,
986 San Diego, CA</bok>

987 <jrn>Mundy CJ, Barber DG, Michel C (2005) Variability of snow and ice thermal, physical and
988 optical properties pertinent to sea ice algae biomass during spring. J Mar Syst 58:107–120
989 doi:10.1016/j.jmarsys.2005.07.003</jrn>

990 <jrn>Mundy CJ, Ehn JK, Barber DG, Michel C (2007) Influence of snow cover and algae on the
991 spectral dependence of transmitted irradiance through Arctic landfast first-year sea ice. J
992 Geophys Res 112:C03007 doi:10.1029/2006JC003683</jrn>

993 <jrn>Nicolaus M, Katlein C, Maslanik J, Hendricks S (2012) Changes in Arctic sea ice result in
994 increasing light transmittance and absorption. Geophys Res Lett 39:L24501
995 doi:10.1029/2012GL053738</jrn>

996 <jrn>Olaizola M, La Roche J, Kolber Z, Falkowski PG (1994) Non-photochemical quenching
997 and the diadinoxanthin cycle in a marine diatom. Photosynth Res 41:357–370 PubMed
998 doi:10.1007/BF00019413</jrn>

999 <jrn>Overland JE, Wang M, Walsh JE, Stroeve JC (2014) Future Arctic climate changes:
1000 adaptation and mitigation time scales. Earths Futur 2:68–74
1001 doi:10.1002/2013EF000162</jrn>

1002 <jrn>Papaioannou G, Papanikolaou N, Retalis D (1993) Relationships of photosynthetically
1003 active radiation and shortwave irradiance. Theor Appl Climatol 48:23–27
1004 doi:10.1007/BF00864910</jrn>

1005 <jrn>Parésys G, Rigart C, Rousseau B, Wong AWM, Fan F, Barbier JP, Lavaud J (2005)
1006 Quantitative and qualitative evaluation of phytoplankton communities by trichromatic
1007 chlorophyll fluorescence excitation with special focus on cyanobacteria. Water Res 39:911–
1008 921 PubMed doi:10.1016/j.watres.2004.12.005</jrn>

1009 <jrn>Parkhill JP, Maillet G, Cullen JJ (2001) Fluorescence-based maximal quantum yield for
1010 PSII as a diagnostic of nutrient stress. J Phycol 37:517–529 doi:10.1046/j.1529-
1011 8817.2001.037004517.x</jrn>

1012 <jrn>Pavlov AK, Taskjelle T, Kauko HM, Hamre B and others (2017) Altered inherent optical
1013 properties and estimates of the underwater light field during an Arctic under-ice bloom of
1014 *Phaeocystis pouchetii*. J Geophys Res 122:4939–4961 doi:10.1002/2016JC012471</jrn>

1015 <jrn>Perovich DK (2005) On the aggregate-scale partitioning of solar radiation in Arctic sea ice
1016 during the Surface Heat Budget of the Arctic Ocean (SHEBA) field experiment. J Geophys
1017 Res 110:C03002 doi:10.1029/2004JC002512</jrn>

1018 <jrn>Petrou K, Ralph PJ (2011) Photosynthesis and net primary productivity in three Antarctic
1019 diatoms: possible significance for their distribution in the Antarctic marine ecosystem. Mar
1020 Ecol Prog Ser 437:27–40 doi:10.3354/meps09291</jrn>

1021 <jrn>Petrou K, Hill R, Brown CM, Campbell DA, Doblin MA, Ralph PJ (2010) Rapid
1022 photoprotection in sea-ice diatoms from the East Antarctic pack ice. Limnol Oceanogr
1023 55:1400–1407 doi:10.4319/lo.2010.55.3.1400</jrn>

1024 <jrn>Petrou K, Hill R, Doblin MA, McMinn A, Johnson R, Wright SW, Ralph PJ (2011)
1025 Photoprotection of sea-ice microalgal communities from the East Antarctic pack ice. J
1026 Phycol 47:77–86 PubMed doi:10.1111/j.1529-8817.2010.00944.x</jrn>

1027 <jrn>Petrou K, Kranz SA, Trimborn S, Hassler CS and others (2016) Southern Ocean
1028 phytoplankton physiology in a changing climate. J Plant Physiol 203:135–150 PubMed
1029 doi:10.1016/j.jplph.2016.05.004</jrn>

1030 <jrn>Poulin M, Daugbjerg N, Gradinger R, Ilyash L, Ratkova T, von Quillfeldt C (2011) The
1031 pan-Arctic biodiversity of marine pelagic and sea-ice unicellular eukaryotes: a first-attempt
1032 assessment. Mar Biodivers 41:13–28 doi:10.1007/s12526-010-0058-8</jrn>

1033 <jrn>Rajanahally MA, Lester PJ, Convey P (2015) Aspects of resilience of polar sea ice algae to
1034 changes in their environment. Hydrobiologia 761:261–275 doi:10.1007/s10750-015-2362-
1035 6</jrn>

1036 <jrn>Ras J, Claustre H, Uitz J (2008) Spatial variability of phytoplankton pigment distributions
1037 in the subtropical South Pacific Ocean: comparison between in situ and predicted data.
1038 Biogeosciences 5:353–369 doi:10.5194/bg-5-353-2008</jrn>

1039 <jrn>Raven JA, Waite AM (2004) The evolution of silicification in diatoms: Inescapable sinking
1040 and sinking as escape? New Phytol 162:45–61 doi:10.1111/j.1469-8137.2004.01022.x</jrn>

1041 <jrn>Renaud PE, Riedel A, Michel C, Morata N, Gosselin M, Juul-Pedersen T, Chiuchiolo A
1042 (2007) Seasonal variation in benthic community oxygen demand: A response to an ice algal
1043 bloom in the Beaufort Sea, Canadian Arctic? J Mar Syst 67:1–12
1044 doi:10.1016/j.jmarsys.2006.07.006</jrn>

1045 <jrn>Richardson K, Beardall J, Raven JA (1983) Adaptation of unicellular algae to irradiance:
1046 an analysis of strategies. New Phytol 93:157–191 doi:10.1111/j.1469-
1047 8137.1983.tb03422.x</jrn>

1048 <jrn>Riedel A, Michel C, Gosselin M, LeBlanc B (2008) Winter–spring dynamics in sea-ice
1049 carbon cycling in the coastal Arctic Ocean. J Mar Syst 74:918–932
1050 doi:10.1016/j.jmarsys.2008.01.003</jrn>

1051 <jrn>Różańska M, Gosselin M, Poulin M, Wiktor JM, Michel C (2009) Influence of
1052 environmental factors on the development of bottom ice protist communities during the
1053 winter–spring transition. Mar Ecol Prog Ser 386:43–59 doi:10.3354/meps08092</jrn>

1054 <jrn>Ryan KG, Ralph P, McMinn A (2004) Acclimation of Antarctic bottom-ice algal
1055 communities to lowered salinities during melting. Polar Biol 27:679–686
1056 doi:10.1007/s00300-004-0636-y</jrn>

1057 <jrn>Ryan KG, Cowie ROM, Liggins E, McNaughtan D, Martin A, Davy SK (2009) The short-
1058 term effect of irradiance on the photosynthetic properties of Antarctic fast-ice microalgal
1059 communities. J Phycol 45:1290–1298 PubMed doi:10.1111/j.1529-8817.2009.00764.x</jrn>

1060 <jrn>Ryan KG, Tay ML, Martin A, McMinn A, Davy SK (2011) Chlorophyll fluorescence
1061 imaging analysis of the responses of Antarctic bottom-ice algae to light and salinity during
1062 melting. J Exp Mar Biol Ecol 399:156–161 doi:10.1016/j.jembe.2011.01.006</jrn>

1063 <jrn>Rysgaard S, Kühl M, Glud RN, Hansen JW (2001) Biomass, production and horizontal
1064 patchiness of sea ice algae in a high-Arctic fjord (Young Sound, NE Greenland). Mar Ecol
1065 Prog Ser 223:15–26 doi:10.3354/meps223015</jrn>

1066 <jrn>Sakshaug E, Slagstad D (1991) Light and productivity of phytoplankton in polar marine
1067 ecosystems: a physiological view. Polar Res 10:69–85 doi:10.3402/polar.v10i1.6729</jrn>

1068 <jrn>Screen JA, Simmonds I (2012) Declining summer snowfall in the Arctic: causes, impacts
1069 and feedbacks. Clim Dyn 38:2243–2256 doi:10.1007/s00382-011-1105-2</jrn>

1070 <jrn>Screen JA, Simmonds I, Keay K (2011) Dramatic interannual changes of perennial Arctic
1071 sea ice linked to abnormal summer storm activity. J Geophys Res 116:D15105
1072 doi:10.1029/2011JD015847</jrn>

1073 <jrn>Sherr EB, Sherr BF, Ross C (2013) Microzooplankton grazing impact in the Bering Sea
1074 during spring sea ice conditions. Deep Sea Res II 94:57–67
1075 doi:10.1016/j.dsr2.2013.03.019</jrn>

1076 <jrn>Singarayer JS, Bamber JL, Valdes PJ (2006) Twenty-first-century climate impacts from a
1077 declining Arctic sea ice cover. J Clim 19:1109–1125 doi:10.1175/JCLI3649.1</jrn>

1078 <jrn>Smith REH, Harrison WG, Harris LR, Herman AW (1990) Vertical fine structure of
1079 particulate matter and nutrients in sea ice of the high Arctic. Can J Fish Aquat Sci 47:1348–
1080 1355 doi:10.1139/f90-154</jrn>

1081 <jrn>Stroeve JC, Serreze MC, Holland MM, Kay JE, Malanik J, Barrett AP (2012) The Arctic's
1082 rapidly shrinking sea ice cover: a research synthesis. Clim Change 110:1005–1027
1083 doi:10.1007/s10584-011-0101-1</jrn>

1084 <jrn>Szechyńska-Hebda M, Kruk J, Górecka M, Karpińska B, Karpiński S (2010) Evidence for
1085 light wavelength-specific photoelectrophysiological signaling and memory of excess light
1086 episodes in *Arabidopsis*. Plant Cell 22:2201–2218 PubMed
1087 doi:10.1105/tpc.109.069302</jrn>

1088 <jrn>Unrein F, Gasol JM, Not F, Fom I, Massana R (2014) Mixotrophic haptophytes are key
1089 bacterial grazers in oligotrophic coastal waters. ISME J 8:164–176 PubMed
1090 doi:10.1038/ismej.2013.132</jrn>

1091 <jrn>Van Heukelem L, Thomas CS (2001) Computer-assisted high-performance liquid
1092 chromatography method development with applications to the isolation and analysis of
1093 phytoplankton pigments. J Chromatogr A 910:31–49 PubMed doi:10.1016/S0378-
1094 4347(00)00603-4</jrn>

1095 <jrn>von Quillfeldt CH, Ambrose WG, Clough LM (2003) High number of diatom species in
1096 first-year ice from the Chukchi Sea. Polar Biol 26:806–818 doi:10.1007/s00300-003-0549-
1097 1</jrn>

1098 <jrn>Wang L, Huang B, Liu X, Xiao W (2015) The modification and optimizing of the
1099 CHEMTAX running in the South China Sea. Acta Oceanol Sin 34:124–131
1100 doi:10.1007/s13131-015-0621-z</jrn>

1101 <jrn>Wassmann P, Duarte CM, Agusti S, Sejr MK (2011) Footprints of climate change in the
1102 Arctic marine ecosystem. Glob Change Biol 17:1235–1249 doi:10.1111/j.1365-
1103 2486.2010.02311.x</jrn>

1104 <jrn>Webster MA, Rigor IG, Nghiem SV, Kurtz NT, Farrell SL, Perovich DK, Sturm M (2014)
1105 Interdecadal changes in snow depth on Arctic sea ice. J Geophys Res 119:5395–5406
1106 doi:10.1002/2014JC009985</jrn>

1107 <jrn>Wilhelm C, Jungandreas A, Jakob T, Goss R (2014) Light acclimation in diatoms: from
1108 phenomenology to mechanisms. Mar Genomics 16:5–15 PubMed
1109 doi:10.1016/j.margen.2013.12.003</jrn>

1110 <jrn>Wright SW, Ishikawa A, Marchant HJ, Davidson AT, van den Enden RL, Nash G (2009)
1111 Composition and significance of picophytoplankton in Antarctic waters. Polar Biol 32:797–
1112 808 doi:10.1007/s00300-009-0582-9</jrn>

1113 <jrn>Wu H, Roy S, Alami M, Green BR, Campbell DA (2012) Photosystem II
1114 photoinactivation, repair, and protection in marine centric diatoms. Plant Physiol 160:464–
1115 476 PubMed doi:10.1104/pp.112.203067</jrn>

1116 <jrn>Yamamoto S, Michel C, Gosselin M, Demers S, Fukuchi M, Taguchi S (2014)
1117 Photosynthetic characteristics of sinking microalgae under the sea ice. Polar Sci 8:385–396
1118 doi:10.1016/j.polar.2014.07.007</jrn>

1119 <jrn>Zapata M, Rodriguez F, Garrido JL (2000) Separation of chlorophylls and carotenoids from
1120 marine phytoplankton: a new HPLC method using a reversed phase C_8 column and pyridine-
1121 containing mobile phases. Mar Ecol Prog Ser 195:29–45 doi:10.3354/meps195029</jrn>

1122 <jrn>Zonneveld C (1998) Photoinhibition as affected by photoacclimation in phytoplankton: a
1123 model approach. J Theor Biol 193:115–123 doi:10.1006/jtbi.1998.0688</jrn>

1124 Table 1. Details of the 3 different experiments conducted during this study. DES: de-epoxidation state; PSII: photosystem II; DTT:
1125 dithiothreitol

Expt	Snow cover	Objective	Period	Light source	Light exposure	Recovery period	Inhibitor treatment
1	Thin and thick	To assess the short-term effect of irradiance range observed at the ice–water interface on the photophysiological response of bottom ice algae	Before and during snow events	Cool white LEDs: 10, 50, 100, 200 μmol m^{-2} s^{-1}	3 h	Yes: 2 h, <5 μmol m^{-2} s^{-1}	No
2	Thin	To determine the respective importance of DES and of the synthesis of PSII D1 protein to support bottom ice algae in maintaining their photochemical performance when exposed to their natural light environment	During snow events	*In situ* irradiance at ice–water interface: from 105 to 53 μmol m^{-2} s^{-1}	6 h	No	Yes: DTT and lincomycin
3	Thin and thick	To assess the photoprotective capability of bottom ice algae when they are exposed to a sudden increase of irradiance	Before snow events	*In situ* irradiance at water surface	3 h	No	No

Table 2. Photosynthetic properties in bottom ice algae acclimated to thin or thick snow cover before and during the snow events. Values are means (±SD) calculated from n samples of the light-use efficiency for low irradiances (α), the relative maximum electron transport rate ($rETR_{max}$) and the light saturation coefficient (E_k)

	Before snow events		During snow events	
Photosynthetic parameter	Thin snow	Thick snow	Thin snow	Thick snow
α (μmol m^{-2} s^{-1})$^{-1}$	0.21 ± 0.04 (n = 7)	0.25 ± 0.11 (n = 6)	0.27 ± 0.05 (n = 16)	0.28 ± 0.09 (n = 22)
$rETR_{max}$ (no units)	7.84 ± 1.61 (n = 7)	3.46 ± 0.75 (n = 7)	7.27 ± 6.08 (n = 18)	7.30 ± 4.63 (n = 22)
E_k (μmol m^{-2} s^{-1})	45.8 ± 8.5 (n = 6)	22.2 ± 11.2 (n = 5)	26.5 ± 15.9 (n = 17)	29.9 ± 13.1 (n = 21)

Fig. 1. Ice camp location (black dot) near Broughton Island (67° 28' N, 63° 47' W). The hamlet of Qikiqtarjuaq is also indicated

Fig. 2. Time series of (a) thin and thick site-averaged snow depth, (b) site-averaged sea ice thickness, (c) nitrate plus nitrite (NO_X) concentration and (d) photosynthetically active radiation (E_{PAR}) transmittance at the ice-water interface during the 3 sampling periods (before and during snow events, and snowmelt). Average was calculated on 9 to 11 values for (a) and (b), and on 2 to 8 values for (d); bars are ±SD

Fig. 3. Time series of (a) total chlorophyll *a* (Tchl *a*) concentration, (b) the ratio of photoprotective (PPC) to photosynthetic carotenoids (PSC) and (c) the ratio of the sum of diadinoxanthin and diatoxanthin (DD+DT) to Tchl *a* under thin and thick snow cover sites during the 3 sampling periods (before and during snow events, and snowmelt). No sampling at thin snow site was performed after 24 June

Fig. 4. Site-averaged relative contribution of major algal groups to chl *a* concentrations (CHEMTAX analysis) under (a) thin and (b) thick snow covers during the 3 sampling periods (before and during snow events and snowmelt). Average was calculated for each snow cover from

8 and 12 samples before and during snow events, respectively. During snowmelt, the average was calculated from 5 samples for thin snow and 9 samples for thick snow

Fig. 5. Maximum quantum yield of PSII photochemistry (F_v/F_m) of bottom ice algae exposed to 10, 50, 100 and 200 µmol photons m^{-2} s^{-1}. Bottom ice algae were collected under (a,c) thin and (b,d) thick snow cover sites (a,b) before and (c,d) during snow events. Samples were exposed to the different light conditions for 3 h, followed by 2 h of recovery at low light (<5 µmol photons m^{-2} s^{-1}). Values are mean ± SD of experiments performed on (a) 14 May (n = 3), (b) 6 and 12 May (n = 6), (c) 25 and 29 May (n = 6) and (d) 27 and 31 May (n = 6)

Fig. 6. De-epoxidation state index (DES = DT / [DD + DT], where DT is diatoxanthin and DD is diadinoxanthin) for bottom ice algae exposed to 10, 50, 100 and 200 µmol photons m^{-2} s^{-1}. Bottom sea ice algae were collected under (a,c) thin and (b,d) thick snow cover sites (a,b) before and (c,d) during snow events, respectively. Samples were exposed to different light conditions for 3 h, followed by 2 h of recovery at low light (<5 µmol photons m^{-2} s^{-1}). Values are averages ± SD of experiments performed on (a) 14 May (n = 3), (b) 6 and 12 May (n = 6), (c) 25 and 29 May (n = 6) and (d) 27 and 31 May (n = 6). Asterisks indicate a significant difference with T_0 of the respective light treatment: *p < 0.05; **p < 0.01; ***p < 0.001

Fig. 7. Variation in (a) estimated photosynthetic active radiation (E_{PAR}) at the ice–water interface, (b) F_v/F_m and (c) DES(see Fig. 6) of bottom ice algae in the presence or absence of the inhibitor of DD de-epoxidation (DTT) and of D1 protein synthesis (lincomycin). Duplicate samples of bottom ice algae were collected under thin snow cover site and exposed to *in situ* irradiance at the ice–water interface from 11:00 to 17:00 h (local time, UTC – 05:00) on 21 May

Fig. 8. Variations in (a) incident PAR, (b) F_v/F_m, (c) total chlorophyll *a* (Tchl *a*) and (d) de-epoxidation state index (DES = DT / [DD + DT], where DT is diatoxanthin and DD is diadinoxanthin) for bottom ice algae exposed to incident irradiance from 12:15 to 15:15 h (local time, UTC – 05:00) on 3 May 2015. E_{PAR} data were not recorded between 14:44 and 15:27 h. Bottom ice algae were collected under thin and thick snow cover sites. In (b–d), values are mean (±SD) calculated from duplicate samples. DES is missing for the thick snow cover site at 15:15 h

Table 1.

Experiment	Snow cover	Objective	Period	Light source	Light exposure	Recovery period	Inhibitor treatment
1	Thin and thick	To assess the short-term effect of irradiance range observed at the ice-water interface on the photophysiological response of bottom ice algae	Before and during snow events	Cool white light-emitting diodes: 10, 50, 100, 200 µmol m^{-2} s^{-1}	3 h	Yes, 2 h, < 5 µmol m^{-2} s^{-1}	No
2	Thin	To determine the respective importance of DES and of the synthesis of PSII D1 protein to support bottom ice algae in maintaining their photochemical performance when exposed to their natural light environment	During snow events	*In situ* irradiance at ice-water interface: from 105 to 53 µmol m^{-2} s^{-1}	6 h	No	Yes: DTT and lincomycin
3	Thin and thick	To assess the photoprotective capability of bottom ice algae when they are exposed to a sudden increase of irradiance	Before snow events	*In situ* irradiance at water surface	3 h	No	No

Table 2.

	Before snow events		During snow events	
Photosynthetic parameter	Thin snow	Thick snow	Thin snow	Thick snow
α (µmol m^{-2} $s^{-1})^{-1}$	0.21 ± 0.04 (n = 7)	0.25 ± 0.11 (n = 6)	0.27 ± 0.05 (n = 16)	0.28 ± 0.09 (n = 22)
$rETR_{max}$ (no unit)	7.84 ± 1.61 (n = 7)	3.46 ± 0.75 (n = 7)	7.27 ± 6.08 (n = 18)	7.30 ± 4.63 (n = 22)
E_k (µmol m^{-2} s^{-1})	45.8 ± 8.5 (n = 6)	22.2 ± 11.2 (n = 5)	26.5 ± 15.9 (n = 17)	29.9 ± 13.1 (n = 21)

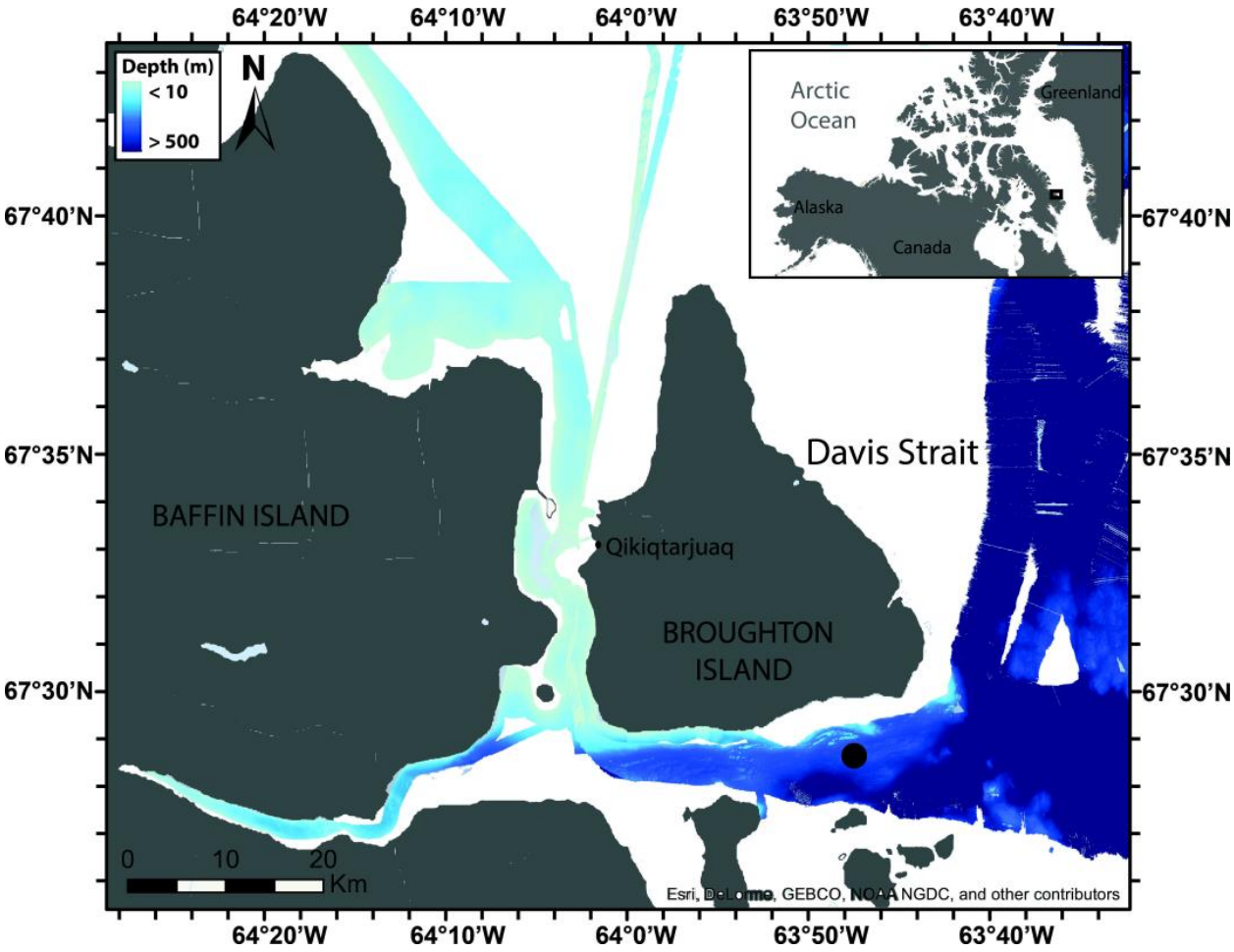
64°20'W
64°10'W
64°0'W
63°50'W
63°40'W
67°40'N
67°35'N
67°30'N
Depth (m)
< 10
> 500
N
Arctic Ocean
Greenland
Alaska
Canada
Davis Strait
BAFFIN ISLAND
Qikiqtarjuaq
BROUGHTON ISLAND
0
10
20
Km
Esri, DeLorme, GEBCO, NOAA NGDC, and other contributors

Figure 1.

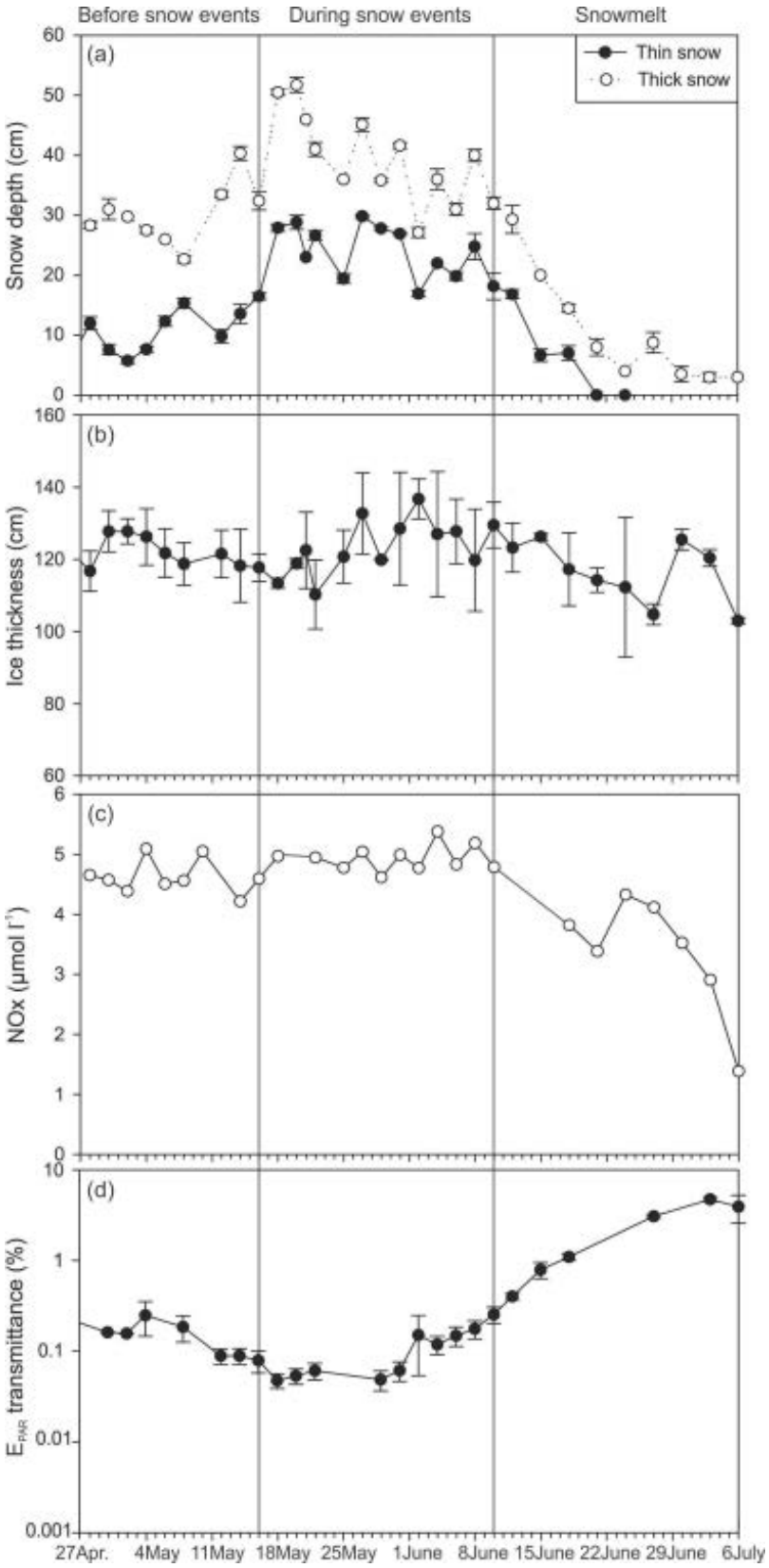
Before snow events
During snow events
Snowmelt
(a)
Thin snow
Thick snow
Snow depth (cm)
(b)
Ice thickness (cm)
(c)
NOx (µmol l⁻¹)
(d)
E_PAR transmittance (%)
27Apr.
4May
11May
18May
25May
1June
8June
15June
22June
29June
6July

Figure 2.

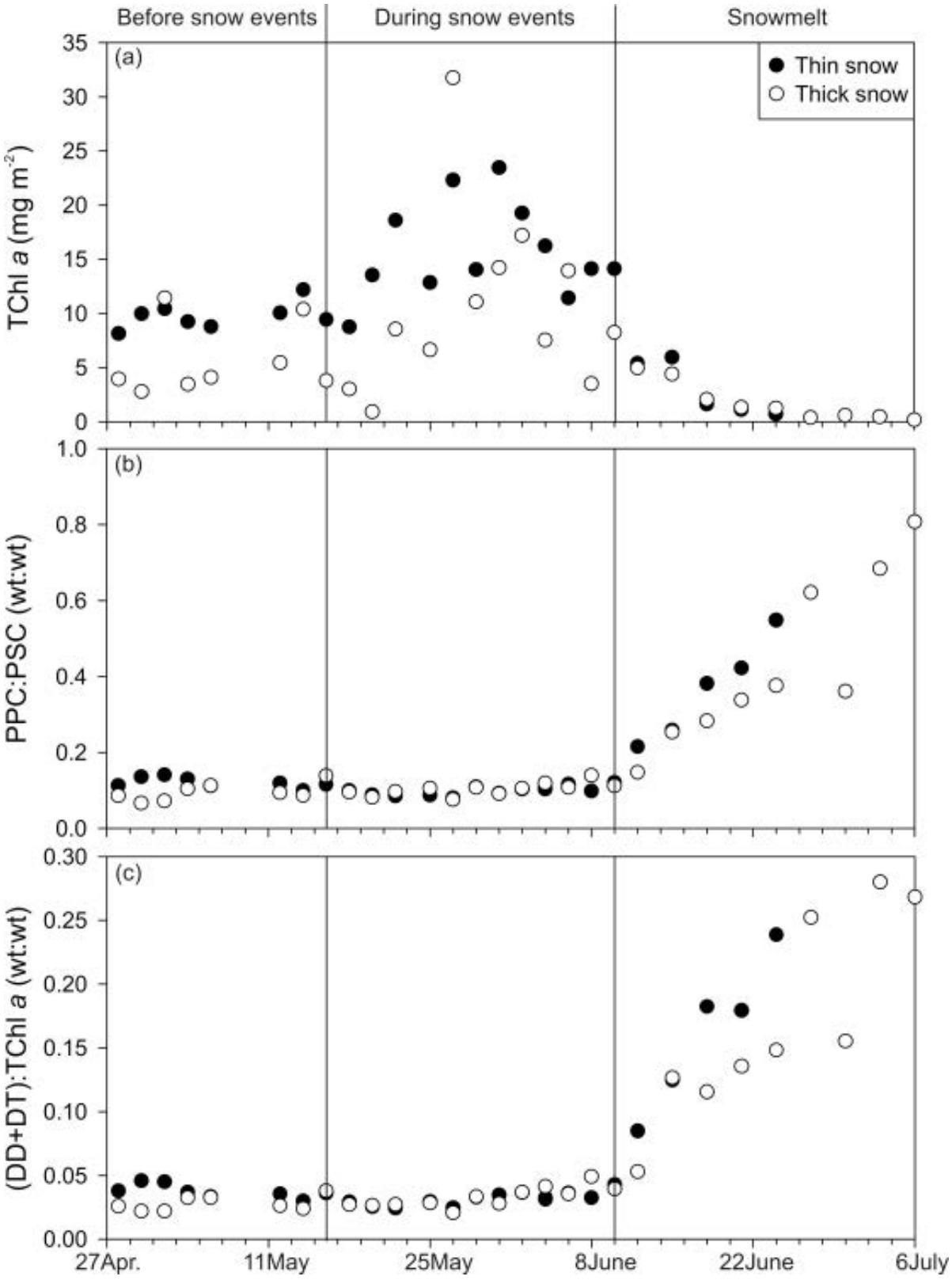
Before snow events
During snow events
Snowmelt
(a)
Thin snow
Thick snow
TChl a (mg m-2)
(b)
PPC:PSC (wt:wt)
(c)
(DD+DT):TChl a (wt:wt)
27Apr.
11May
25May
8June
22June
6July

Figure 3.

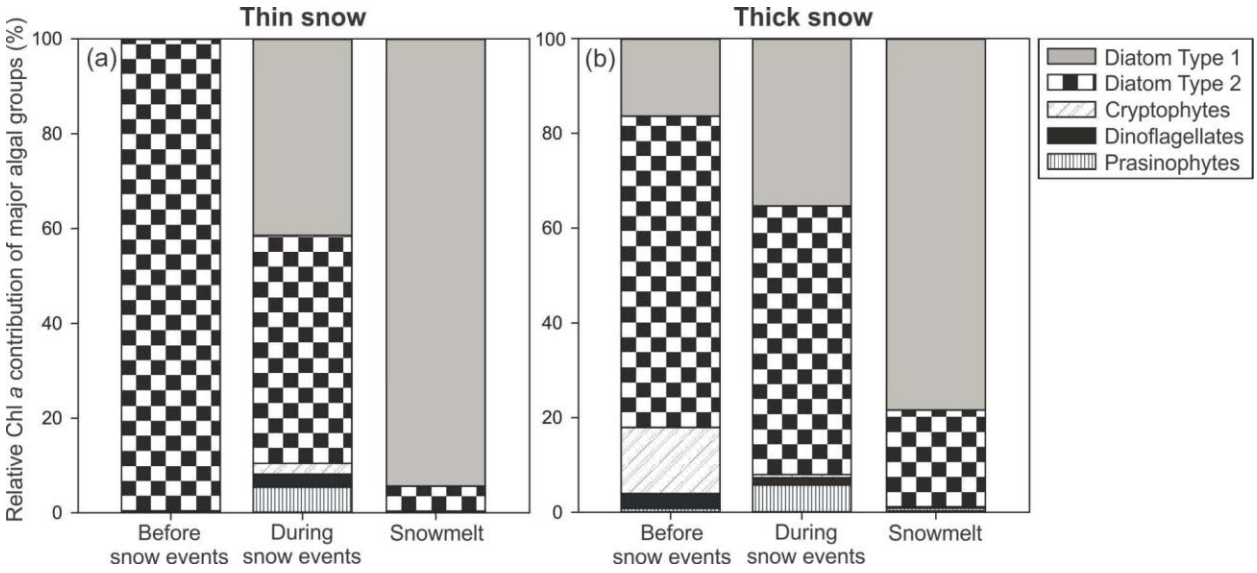
Thin snow
Thick snow
(a)
(b)
Relative Chl a contribution of major algal groups (%)
0
20
40
60
80
100
Before snow events
During snow events
Snowmelt
Diatom Type 1
Diatom Type 2
Cryptophytes
Dinoflagellates
Prasinophytes

Figure 4.

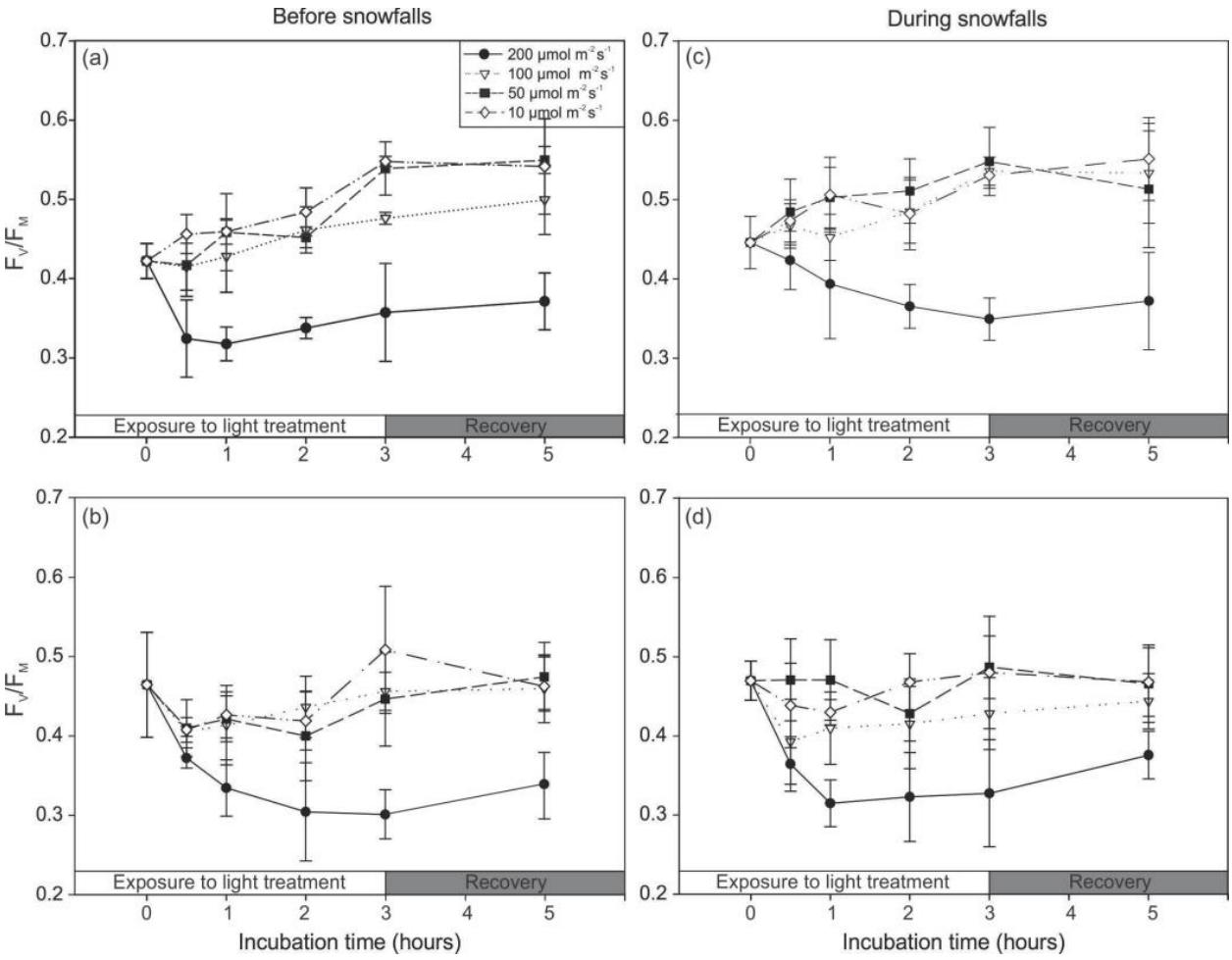
Before snowfalls
During snowfalls
(a)
(b)
(c)
(d)
200 µmol m-2s-1
100 µmol m-2s-1
50 µmol m-2s-1
10 µmol m-2s-1
FV/FM
Exposure to light treatment
Recovery
Incubation time (hours)

Figure 5

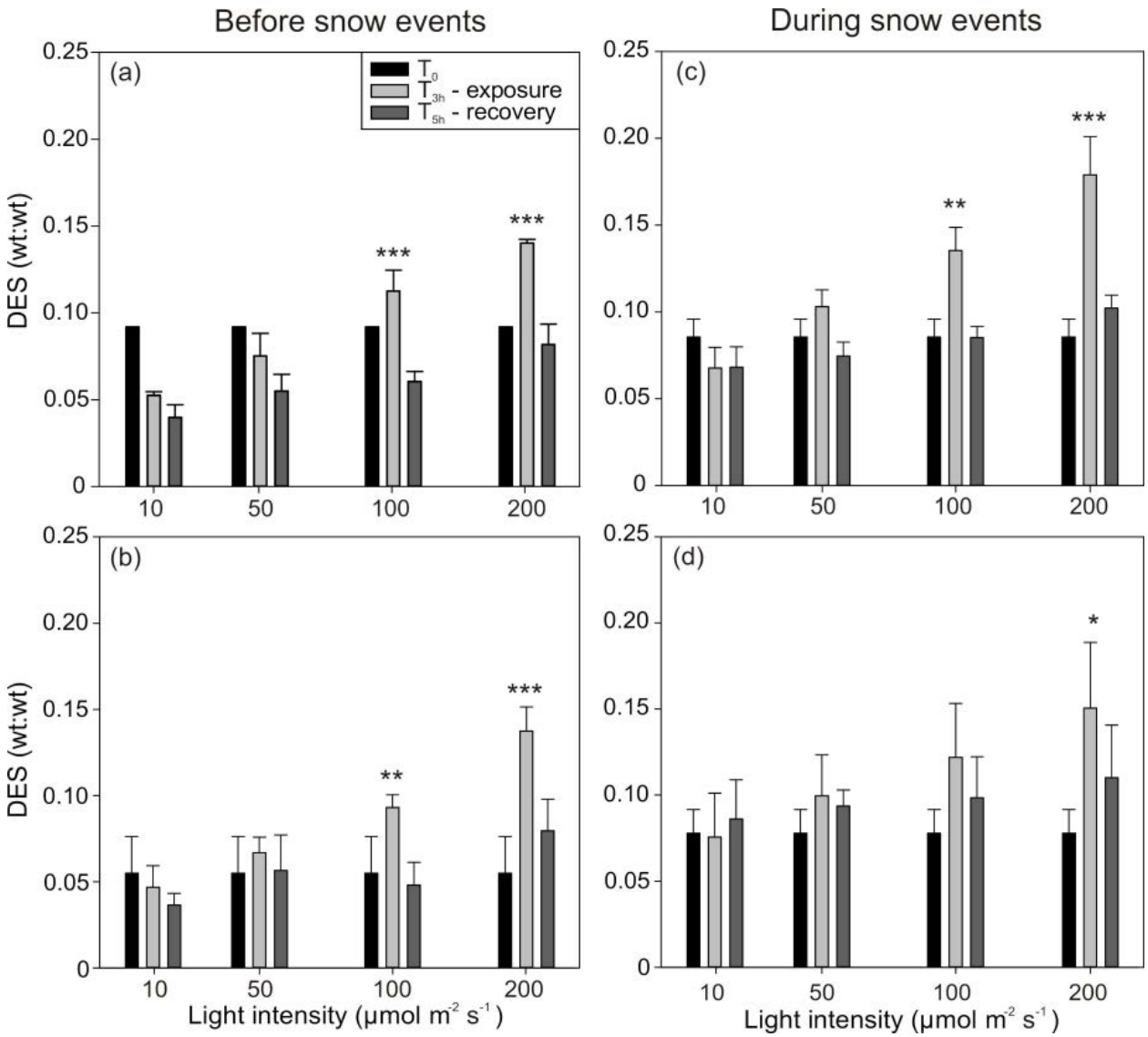
Before snow events
During snow events
(a)
(b)
(c)
(d)
T_0
T_{3h} - exposure
T_{5h} - recovery
DES (wt:wt)
Light intensity (µmol m^{-2} s^{-1})
0.25
0.20
0.15
0.10
0.05
0
10
50
100
200
***
**
*

Figure 6.

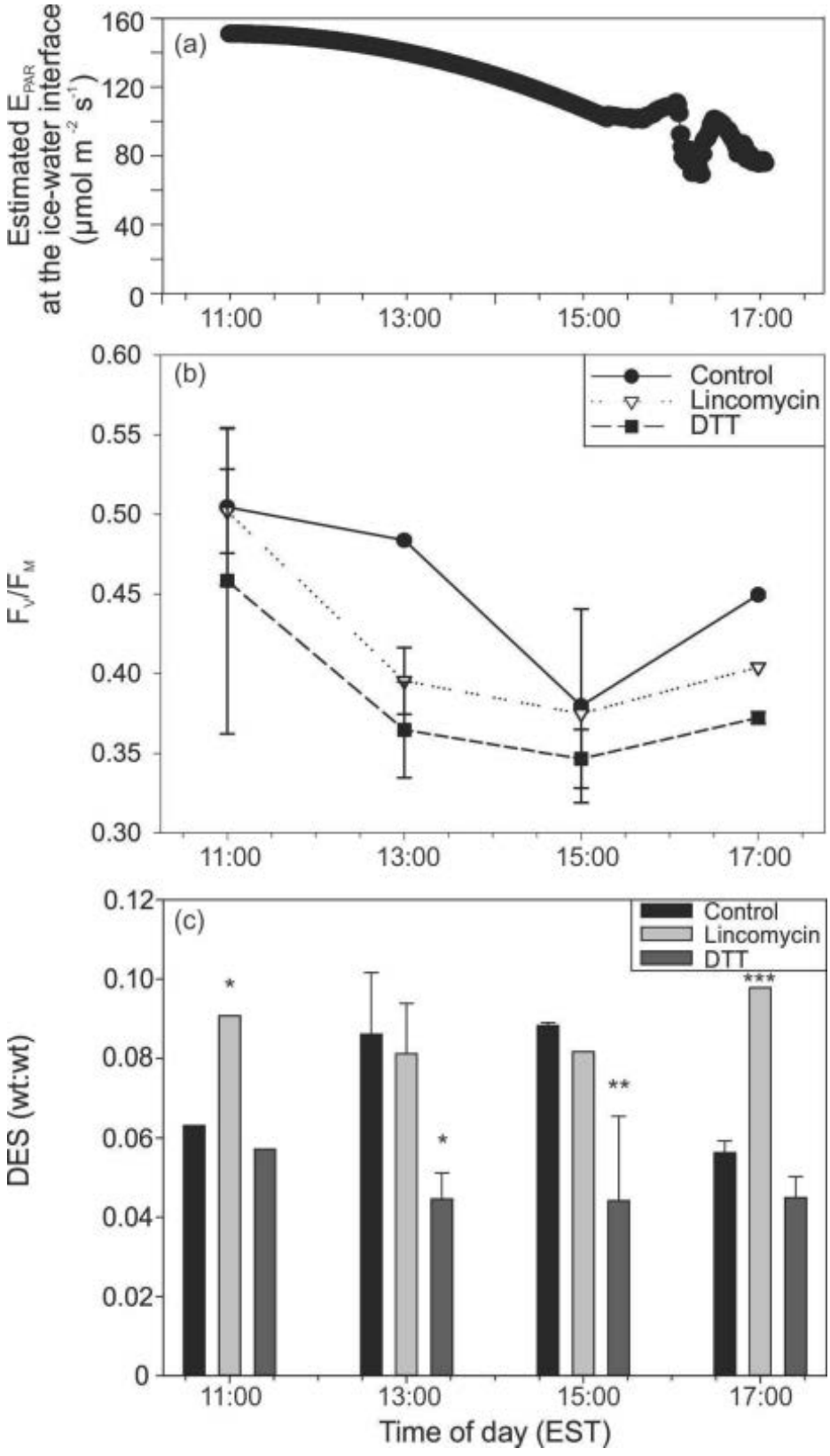
(a)
Estimated E_{PAR} at the ice-water interface (µmol m^{-2} s^{-1})
160
120
80
40
0
11:00
13:00
15:00
17:00
(b)
Control
Lincomycin
DTT
F_V/F_M
0.60
0.55
0.50
0.45
0.40
0.35
0.30
11:00
13:00
15:00
17:00
(c)
Control
Lincomycin
DTT
DES (wt:wt)
0.12
0.10
0.08
0.06
0.04
0.02
0
*
*
**
***
11:00
13:00
15:00
17:00
Time of day (EST)

Figure 7.

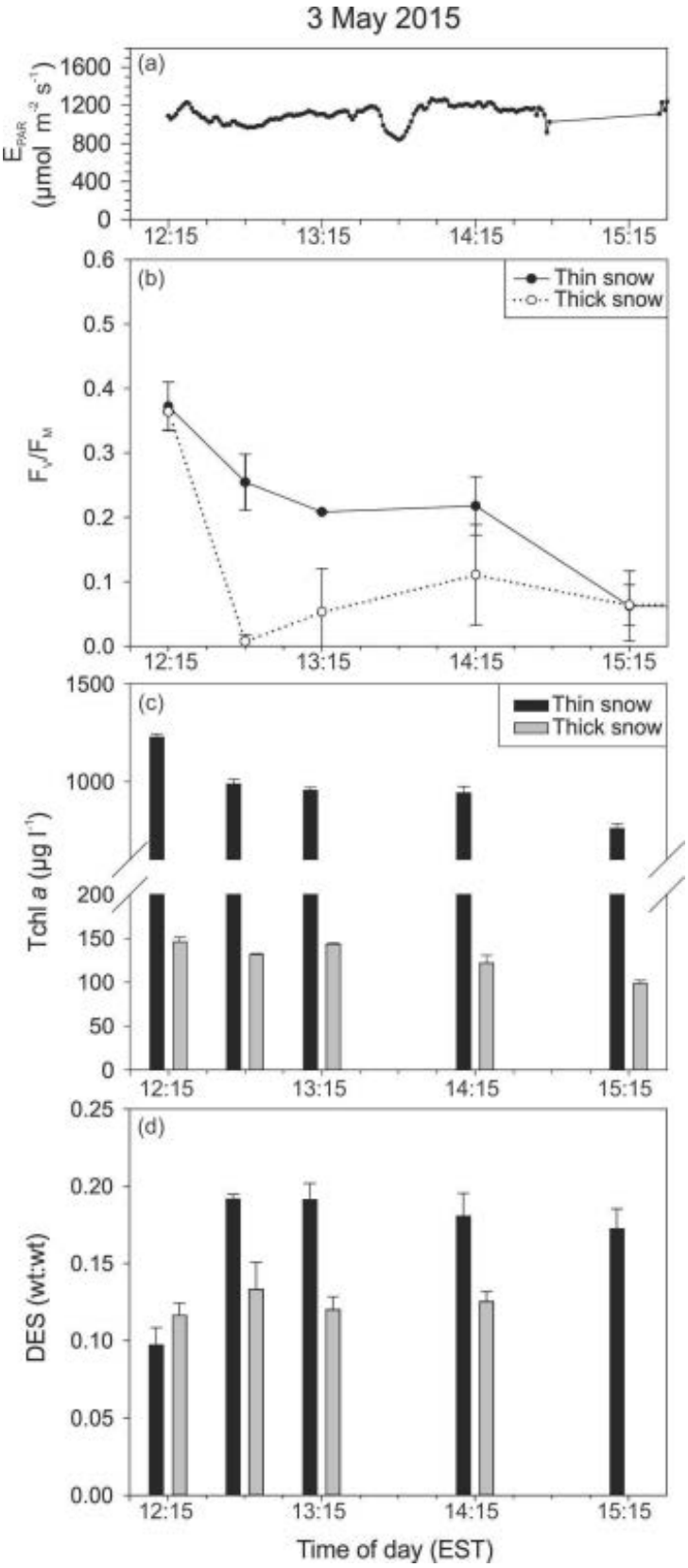
3 May 2015
(a)
E_{PAR} (µmol m^{-2} s^{-1})
1600
1200
800
400
0
12:15
13:15
14:15
15:15
(b)
Thin snow
Thick snow
F_v/F_M
0.6
0.5
0.4
0.3
0.2
0.1
0.0
(c)
Thin snow
Thick snow
Tchl *a* (µg l^{-1})
1500
1000
200
150
100
50
0
(d)
DES (wt:wt)
0.25
0.20
0.15
0.10
0.05
0.00
Time of day (EST)

Figure 8